2012321

Data Repository for:
Owyhee River Intracanyon Lava Flows: Does the River Give a Dam?

Lisa L. Ely, Cooper C. Brossy, P. Kyle House, Elizabeth B. Safran, Jim E. O'Connor, Duane E. Champion, Cassandra R. Fenton, Ninad R. Bondre, Caitlin A. Orem, Gordon E. Grant, Christopher D. Henry, Brent D. Turrin

Ages of Lava Flows and Associated Erosional and Depositional Features

The six sets of lava flows that entered the Owyhee River canyon were distinguished and assigned relative and absolute ages through a combination of field, laboratory and analytical methods (Table 1, main text). Field observations included surface morphology, amount of soil development and weathering, hand sample mineralogy (Table DR 4; Brossy, 2007), geomorphic location in the canyon, and stratigraphic position. The ages of the lava dams and associated features were determined using $^{40}Ar/^{39}Ar$ radiometric dating of the basalt flows, cosmogenic ^{3}He surface-exposure ages of lava flows and boulders, tephrochronology of lacustrine and landslide sediments, and remanent paleomagnetic analysis of the lava flows (Table DR 1), as detailed in the following sections. Lava flows within the canyon were further correlated to each other and to source vents using major and trace-element geochemical analyses (Fig. DR 1) and remanent paleomagnetic signatures (Table DR 3, Fig. DR 2).

Samples for $^{40}Ar/^{39}Ar$ radiometric ages were analyzed at Rutgers University Department of Earth and Planetary Sciences, the New Mexico Geochronology Research Laboratory at the New Mexico Institute of Mining and Technology, and the Nevada Isotope Geochronology Laboratory at the University of Nevada, Las Vegas using standard procedures for each laboratory. The Data Repository includes commentary relevant to specific $^{40}Ar/^{39}Ar$ radiometric age interpretations, as well as the full analytical results (Tables DR 5, DR 6 and DR 7; Figs. DR 3, DR 4 and DR 5). The data evaluation protocol used here is based on Fleck et al. (1977), and Dalrymple and Lanphere (1969, 1974).

We conducted cosmogenic radionuclide surface-exposure analyses on the youngest of the Owyhee River lava dams, the West Crater lava dam (70 ka, Table DR 1), and associated river-eroded channels, strath terraces, and boulder deposits. The surface-exposure ages were determined through the analysis of cosmogenic ^{3}He, henceforth referred to as $^{3}He_c$ (Tables DR 1 and DR 2). Samples for cosmogenic dating were collected and prepared according to the methods described by Gosse and Phillips (2001) and Fenton et al. (2002, 2004). Analyses were completed at the University of Rochester and the US Geological Survey in Denver. The cosmogenic ^{3}He surface-exposure ages were calculated using (1) The SLHL 3He production rate of 115 at/g/yr (Cerling and Craig, 1994), and (2) T. Cerling's fit to Lal's (1991) scaling scheme. Cerling's scaling factors are 2–3% higher than those calculated for the commonly used Lal (1991) scaling scheme by CosmoCalc (Vermeesch, 2007; Fenton et al., 2009).

The representative age for each lava flow used in the text (Tables 1 and 2) is based on a weighted mean average and standard error of the most reliable geochronological information available for each lava flow. Individual determinations were weighted by the inverse of their squared uncertainties (standard deviations) and summed. The uncertainty of the weighted mean is the reciprocal square root of the sum of all the individual weights (Taylor, 1982). The inclusion or exclusion of sample age results from the calculations of the representative weighted mean ages was based on our confidence in the quality of the sample, the stratigraphic or geologic relation to other geologic units of known ages, and the degree of analytical uncertainty. We preferentially used the plateau ages from the $^{40}Ar/^{39}Ar$ experiments whenever the isochron intercepts suggest that is appropriate.

The rationale for the selection of samples for each representative age calculation is below:.

Lower Bogus lavas: No single representative age was calculated because the number and stratigraphic relations of the individual flows is uncertain. The minimum age is constrained by the $^{40}Ar/^{39}Ar$ age of 1.672 ± 0.03 Ma on an upper flow unit (Sample #9429B). Another age of 1.92±0.011 (Bondre, 2006) from a vent east of Bogus Rim is probably from one of the lower Bogus lavas. Ages of 1.86 and 1.87 Ma (Bondre, 2006) were derived from lava flows that issued from Owyhee Butte (Fig. 2). Although not part of the lower Bogus lava group, these flows appear to have entered a lake formed behind one of the lower Bogus lava dams. Based on these results, we estimated an approximate age range of 1.7-2 Ma for the lower Bogus lavas. The age of 1.01 ±0.139 Ma (Sample #3419B) at Bogus Point is an outlier when compared with geochronological results from the lower Bogus lavas and the Bogus Rim lava flow at other locations. Because of the ambiguous stratigraphic relation between the Bogus Point outcrop and the other lower Bogus and Bogus Rim lava flows, the results from this sample were not included in the overall age estimate.

Bogus Rim lava flow: A high-quality sample from the uppermost unit of the lower Bogus lava group yielded an $^{40}Ar/^{39}Ar$ age of 1.67 ±0.03 Ma. The dated unit directly underlies the Bogus Rim lava flow, thus providing a maximum limiting age. The reversed magnetic polarity of the Bogus Rim lava flow indicates that it is younger than 1.77 Ma. These two ages were combined to determine the representative age of 1.7 Ma.

Deer Park lava flow: Only one $^{40}Ar/^{39}Ar$ age of 780 ± 50 was obtained from the Deer Park lava flow, so it was used as the representative age. The result is consistent with the reversed magnetic polarity of this lava flow, which would place the age as ≥780 ka.

Clarks Butte lava flow: The three available $^{40}Ar/^{39}Ar$ ages were used to calculated the weighted mean. The isochron age for sample OWY-35 was selected over the plateau age because it had a lower analytical error.

Saddle Butte lava flows: The $^{40}Ar/^{39}Ar$ age of 144±14 ka on sample 428B4 was used as the representative age for these lava flows. It was from a high-quality sample and the analytical uncertainty was low, so we have a high degree of confidence in the resulting age (Fig. DR3; Table DR5). The other two available $^{40}Ar/^{39}Ar$ ages were excluded from the weighted mean. The large analytical error for sample OWY-12 and the unrealistically old age of 7 Ma for sample OWY-13 contradict the known stratigraphic and geologic position of this unit.

West Crater lava flow: The weighted mean was calculated using Samples JV99-1, N17/03 (Bondre, 2006), and the plateau values for OWY-22 and OWY-23. The plateau values were used for the latter two samples because the isochron value for OWY-22 contradicts the ages derived from all other geochronological methods and the isochron age for OWY-23 had a very large analytical error. Sample OWY-36 was excluded because of our low confidence in the reliability of the $^{40}Ar/^{39}Ar$ total gas analytical procedure.

Cosmogenic radionuclide surface exposure ages on West Crater lava flow and boulders: All available results from each surface or boulder were used to calculate the weighted mean for that feature, with one exception. Sample 042904-34 was excluded from the weighted mean age of the slighted eroded West Crater lava flow top at Dogleg Bend terrace T5. Analysis of aerial photographs revealed that the surface from which this sample was collected might have been mobilized or previously covered by a landslide, and could not be confidently interpreted as an undisturbed surface of the lava flow.

Table DR1. Age analyses of lava flows and associated features. Full analytical results are in Tables DR 2 through 7.

Lava Flow/ Sample/ Location	Age[a] (ka)	Method	Sample Coordinates[b]		Source
			Latitude (°N)	Longitude (°W)	
Undivided Lower Bogus Lavas					
9429B, Immediately underlies Bogus Rim lava near Rinehart Ranch; used to calculate weighted mean age of Bogus Rim lava	1672 ± 30	$^{40}Ar/^{39}Ar$ plateau	43.206	117.632	This study
[c]3419B, At Bogus Point	1010 ± 139	$^{40}Ar/^{39}Ar$ plateau	43.057	117.646	This study
N6/04, Bogus Bench near source	1920 ± 110	$^{40}Ar/^{39}Ar$ plateau	43.07958	117.55314	Bondre, 2006
N9/03, Owyhee Butte (not part of the lower Bogus lava group, but flowed into a lake formed by a lower Bogus lava dam)	1860 ± 115	$^{40}Ar/^{39}Ar$ plateau	42.95042	117.63867	Bondre, 2006
N9/04, (not part of lower Bogus lava group, but contemporaneous with Owyhee Butte)	1870 ± 40	$^{40}Ar/^{39}Ar$ plateau	42.92120	117.65184	Bondre, 2006
Bogus Rim Lava					
[d]Representative Age (younger than Sample 9429B above)	**≤1692 ± 30 (1700)**				
Dear Park Lavas					
[d]Representative Age	**780 ± 50 (780)**				
446B7, SW of Hill 4737	>778 (reversed polarity)	Paleomag.	43.161	117.513	Champion, this study
429B7, Within canyon	780 ± 50	$^{40}Ar/^{39}Ar$ plateau	43.198	117.548	This study
Clarks Butte Lava Flow					
[d]Representative Weighted Mean Age (Samples: Clarks Butte Shield, OWY-35 isochron, 0428B)	**214±9 (215)**				
Clarks Butte Shield	250 ± 50	K-Ar	N.D.	N.D.	Hart and Mertzman, 1983
[c]OWY-35, upper AM-PM outcrop	248 ± 25	$^{40}Ar/^{39}Ar$ plateau	43.13138	117.70269	This study
[c]OWY-35, upper AM-PM outcrop	179 ± 21	$^{40}Ar/^{39}Ar$ isochron	43.13138	117.70269	This study
0428B, upper AM-PM outcrop	220 ± 10	$^{40}Ar/^{39}Ar$ plateau	43.134	117.708	This study
Saddle Butte Lava Field					
[d]Representative Age (Sample 428B4)	**144 ± 14 (145)**				
428B4, Highway 78 road cut	144 ± 14	$^{40}Ar/^{39}Ar$ plateau	42.957	118.049	B. Turrin, this study

Table DR1. Age analyses of lava flows and associated features. Full analytical results are in Tables DR 2 through 7.

Lava Flow/ Sample/ Location	Age[a] (ka)	Method	Sample Coordinates[b]		Source
			Latitude (°N)	Longitude (°W)	
[c]OWY-12, Saddle Butte 1	173 ± 145	$^{40}Ar/^{39}Ar$ plateau	43.01049	117.71742	This study
[c]OWY-13, Saddle Butte 2	7000 ± 1000	$^{40}Ar/^{39}Ar$ plateau	43.01073	117.71836	This study
West Crater Lava Flow					
[d]Representative Weighted Mean Age (Samples JV99-1; N17/03; OWY-22 and OWY-23 plateaus)	**69±9 (70)**				
JV99-1	61 ± 12	$^{40}Ar/^{39}Ar$ isochron	43.06270	117.65139	Bondre, 2006
N17/03	86 ± 17	$^{40}Ar/^{39}Ar$ isochron	43.00021	117.55061	Bondre, 2006
[c]OWY-22, upper West Crater	38 ± 21	$^{40}Ar/^{39}Ar$ plateau	43.09241	117.70799	This study
[c]OWY-22, upper West Crater	7 ± 8.5	$^{40}Ar/^{39}Ar$ isochron	43.09241	117.70799	This study
[c]OWY-23, lower West Crater	182 ± 42	$^{40}Ar/^{39}Ar$ plateau	43.09532	117.70653	This study
[c]OWY-23, lower West Crater	120 ± 130	$^{40}Ar/^{39}Ar$ isochron	43.09532	117.70653	This study
[c]OWY-36, lower West Crater	194 ± 27	$^{40}Ar/^{39}Ar$ total gas	43.13226	117.70055	This study
Boulders on dam surface	**62 ± 3**	Weighted mean			Samples 090506-14, -15, -16
090506-14[e], boulder on dam surface	67 ± 5	$^{3}He_c$	43.0934	117.7096	Fenton, this study
090506-15[e], boulder on dam surface	62 ± 4	$^{3}He_c$	43.0934	117.7096	Fenton, this study
090506-16[e], boulder on dam surface	58 ± 4	$^{3}He_c$	43.0934	117.7096	Fenton, this study
Airplane Point; polished, eroded surface of West Crater lava dam	**39 ± 2**	Weighted mean			Samples 090506-17, -18, -19, -21
090506-17[f], Airplane Point, upper	36 ± 3	$^{3}He_c$	43.1187	117.7053	Fenton, this study
090506-18 [f], Airplane Point, lower	34 ± 2	$^{3}He_c$	43.1184	117.7054	Fenton, this study
090506-19[f], Airplane Point, lower	64 ± 5	$^{3}He_c$	43.1189	117.7053	Fenton, this study
090506-21[f], Airplane Point, lower	44 ± 3	$^{3}He_c$	43.1189	117.7053	Fenton, this study
Dogleg Bend surfaces eroded into West Crater lava dam					
T5, slightly eroded flow top	**58 ± 3**	Weighted mean			Samples 042904-17 and -18
042904-17[g], slightly eroded flow top	58 ± 4	$^{3}He_c$	43.1096	117.7190	Fenton, this study
042904-18[g], slightly eroded flow top	57 ± 4	$^{3}He_c$	43.1096	117.7190	Fenton, this study
042904-34[g, h] lava, possibly a landslide block or covered by a landslide for a period of time	41 ± 3	$^{3}He_c$	43.1089	117.7120	Fenton, this study
T5 strath boulders	**45 ± 3**	Weighted mean			Samples 042901-19, -20, -21, -22

Table DR1. Age analyses of lava flows and associated features. Full analytical results are in Tables DR 2 through 7.

Lava Flow/ Sample/ Location	Age[a] (ka)	Method	Sample Coordinates[b]		Source
			Latitude (°N)	Longitude (°W)	
042904-19 [e], boulder onT5 strath	69 ± 5	^3He_c	43.1096	117.7190	Fenton, this study
042904-20[e], boulder onT5 strath	45 ± 3	^3He_c	43.1096	117.7190	Fenton, this study
042904-21 [e], boulder onT5 strath	42 ± 3	^3He_c	43.1096	117.7190	Fenton, this study
042904-22 [e], boulder onT5 strath	38 ± 3	^3He_c	43.1096	117.7190	Fenton, this study
T4 strath boulders	**39 ± 3**	Weighted mean			Samples 042901-23 and -24
042904-23 [e], boulder onT4 strath	41 ± 3	^3He_c	43.1102	117.7206	Fenton, this study
042904-24 [e], boulder onT4 strath	36 ± 3	^3He_c	43.1102	117.7206	Fenton, this study
T3 boulders	**17 ± 1**	Weighted mean			Samples 042904-26, -27, -29
042904-26 [e], T3 boulder terrace	19 ± 1	^3He_c	43.1101	117.7220	Fenton, this study
042904-27 [e], T3 boulder terrace	17 ± 1	^3He_c	43.1101	117.7220	Fenton, this study
042904-29 [e], T3 boulder terrace	14 ± 1	^3He_c	43.1101	117.7220	Fenton, this study
T2 boulders	**12 ± 1**	Weighted mean			Samples 042904-30, -31, -32
042904-30 [e], T2 boulder terrace	12 ± 1	^3He_c	43.1087	117.7216	Fenton, this study
042904-31 [e], T2 boulder terrace	11 ± 1	^3He_c	43.1087	117.7216	Fenton, this study
042904-32 [e], T2 boulder terrace	12 ± 1	^3He_c	43.1087	117.7216	Fenton, this study
T1 boulders	**9 ± 1**	Weighted mean			Samples 043004-35, -36, -38
043004-35 [e], T1 boulder terrace	38 ± 3	^3He_c	43.1082	117.7188	Fenton, this study
043004-36 [e], T1 boulder terrace	6 ± 1	^3He_c	43.1082	117.7188	Fenton, this study
043004-38 [e], T1 boulder terrace	9 ± 1	^3He_c	43.1082	117.7188	Fenton, this study
Tephra in lake sediments behind West Crater dam[i]					
9120707, MSH C_y, rt. bank	47± 5	Tephra	43.06258	117.68574	This study
4270801, MSH C_y, rt. bank	47± 5	Tephra	43.07067	117.68620	This study
4270801cb, MSH C_y or C_w, left bank	47± 5 or 49-55	Tephra	43.06643	117.69668	This study
CAO-OW-0609-BH-1, MSH C_w, rt. bank	49-55	Tephra	43.0652	117.6839	This study
CAO-OW-0609-CH-53, MSH C_w, rt. bank	49-55	Tephra	43.0627	117.6849	This study
CAO-OW-0709-MWC-2, MSH C_w or C_y, left bank	47± 5 or 49-55	Tephra	43.0625	117.6941	This study
Other associated tephra deposits					
7170802 Trego Hot Springs tephra, closed depression on landslide whose toe is buried by WC lava	23.2	Tephra	42.79389	117.71290	This study

Table DR1. Age analyses of lava flows and associated features. Full analytical results are in Tables DR 2 through 7.

Lava Flow/ Sample/ Location	Age[a] (ka)	Method	Sample Coordinates[b]		Source
			Latitude (°N)	Longitude (°W)	
Mazama tephra, same auger hole as 7170802, above	7.7	Tephra	42.79389	117.71290	This study
OW-042804-04 Mazama tephra in closed depression, Artillery landslide	7.7	Tephra	43.02332	117.68865	This study
[j]CAO-OW-0609-WCT-2, Summer Lake LL tephra at base of lake sediments on or adjacent to WC dam top	160 ± 35	Tephra	43.0687	117.6809	This study

Note: N.D.—no data. $^{3}He_{c}$—^{3}Helium cosmogenic exposure dating. WC—West Crater lava flow.

[a] 1-sigma uncertainty reported for $^{40}Ar/^{39}Ar$ ages.
[b] Coordinates are WGS84 datum.
[c] Complications arose in the application of the $^{40}Ar/^{39}Ar$ analytical procedure on these young basalts. The results of these analyses were inconsistent with field relations and other ages or had analytical uncertainties that deemed them of minimal value for geologic interpretation.
[d] The representative ages for each lava flow or group of cosmogenic surface exposure ages are weighted mean averages of the relevant geochronological data available for each. Individual determinations weighted by the inverse of their squared uncertainties (standard deviations) and summed. The uncertainty of the weighted mean is the reciprocal square root of the sum of all the individual weights. The Data Repository text includes explanations of which samples were used and excluded from the calculations of the representative ages.
[e] Samples were collected from the upper surfaces of basalt boulders transported by fluvial processes (e.g. boulder bars, boulders on strath terraces, etc.).
[f] Samples were collected from the surfaces of river-polished, in-situ basalt of the West Crater lava flow.
[g] Sample collected from a lava flow surface (e.g. pahoehoe, tumuli or other primary flow surfaces).
[h] Aerial photos indicate that this sample is either a landslide block that fell onto the West Crater flow surface, or it was covered by landslide debris for a period of time; result is a minimum age for the WC lava
[i] Analyzed for geochemical match with the regional tephra database at the Geoanalytical Lab at Washington State University. The most likely ages for Mt. St. Helens C_w and C_y tephras were determined by Orem (2010) from a compilation of sources (Berger and Busacca, 1995; Negrini et al., 2000; Clynne et al., 2008).
[j] Sample CAO-OW-0609-WCT-2 is from the base of a small, isolated section of fine-grained sediments that are adjacent to and at an elevation equivalent to the top of the West Crater dam. The stratigraphic relation to the WC dam is ambiguous. This section could be older than the West Crater lava flow or the geochemical correlation to Summer Lake LL tephra (Davis, 1985; Negrini et al., 2000) could be incorrect.

Table DR 2. $^{3}He_{c}$ exposure age data from olivine separates in the Owyhee River region, Oregon.

Location/Sample	Sample Thickness (cm)	Mass (g)	R/R_a [a] fusion	^{4}He content (10^{9} atoms/g) [b]	Uncertainty of ^{4}He content (10^{9} atoms/g) [b]	$^{3}He_{c}$ content [b,c] (10^{6} atoms/g) z=0 cm	Uncertainty of ^{3}He content (10^{6} atoms/g) [b]	Cerling Scaling Factor (Fenton et al., 2009)	Production rate [d] (atoms/g/yr)	Cosmogenic ^{3}He age (ka)	Uncertainty [e] (ka)
042904-17 [f]	4	0.1005	30.56	330.91	16.55	14.56	0.73	2.26	250	58	4
042904-18 [f]	4	0.0974	144.24	69.16	3.46	14.36	0.72	2.26	250	57	4
042904-19 [g]	4	0.1058	30.95	385.90	19.29	17.19	0.86	2.26	250	69	5
042904-20 [g]	4	0.2208	196.21	38.63	1.93	10.91	0.55	2.26	246	45	3
042904-21 [g]	4	0.3691	98.17	72.46	3.62	10.24	0.51	2.26	246	42	3
042904-22 [g]	4	0.2977	99.39	66.97	3.35	9.58	0.48	2.26	246	38	3
042904-23 [g]	4	0.2904	76.35	88.88	4.44	9.77	0.49	2.23	243	41	3
042904-24 [g]	4	0.3049	96.64	63.49	3.17	8.83	0.44	2.23	243	36	3
042904-26 [g]	4	0.3103	35.18	87.69	4.38	4.44	0.22	2.21	240	19	1
042904-27 [g]	4	0.2585	37.31	73.17	3.66	3.93	0.20	2.21	240	17	1
042904-29 [g]	4	0.2530	33.87	66.65	3.33	3.25	0.16	2.21	240	14	1
042904-30 [g]	4	0.2036	24.04	84.50	4.22	2.92	0.15	2.20	239	12	1
042904-31 [g]	4	0.1961	22.26	87.53	4.38	2.80	0.14	2.20	239	11	1
042904-32 [g]	4	0.3110	59.26	34.95	1.75	2.98	0.15	2.20	239	12	1
042904-34 [f]	4	0.3103	106.43	66.97	3.35	10.26	0.51	2.30	250	41	3
043004-35 [g]	4	0.1003	101.68	62.14	3.11	9.09	0.45	2.17	238	38	3
043004-36 [g]	4	0.1046	16.88	65.54	3.28	1.59	0.08	2.17	236	6	0
043004-38 [g]	4	0.1000	29.76	51.29	2.56	2.20	0.11	2.17	236	9	1
090506-14 [g]	4	0.1079	33.19	356.65	17.83	17.04	0.85	2.31	256	67	5
090506-15 [g]	4	0.1042	23.36	472.64	23.63	15.89	0.79	2.31	256	62	4
090506-16 [g]	4	0.1004	27.40	375.86	18.79	14.82	0.74	2.31	256	58	4
090506-17 [h]	5	0.1022	132.83	46.02	2.30	8.88	0.44	2.20	239	36	3
090506-18 [h]	5	0.1015	111.98	50.93	2.55	8.29	0.41	2.20	239	34	2
090506-19 [h]	4	0.0998	25.78	420.93	21.05	15.62	0.78	2.20	241	64	5
090506-21 [h]	5	0.0991	132.30	54.56	2.73	10.49	0.52	2.20	239	44	3
Shielded Sample (contains only non-cosmogenic helium)											
043004-01DC		0.3077	2.27								

Table DR2 Notes:

[a] R_a=1.384x10^{-6}. R/R_a values corrected for background blank and air $^3He/^4He$ content. Values are also corrected with the $^3He/^4He$ value of a shielded sample (043004-01DC) collected at 2 m depth from a cave under the West Crater lava flow at Dogleg Bar. The shielded sample is assumed to contain only non-cosmogenic $^3He/^4He$ with a measured R/Ra value of 2.27.

[b] Analytical error ≤ 5%; includes corrections for precision of mass spectrometer, blanks and standards.

[c] ^3He_c atom concentration corrected to the surface of each sample (i.e. z = 0 cm), accounting for self–shielding.

[d] Production rate is corrected for skyline shielding resulting from surrounding topography.

[e] Uncertainty (1σ) includes error propagation of analytical error and production rate uncertainty.

[f] Sample collected from a lava flow top (e.g. pahoehoe, tumuli and other primary flow surfaces).

[g] Samples were collected from the upper surfaces of basalt boulders transported by fluvial processes (e.g. boulder bars, boulders on strath terraces, etc.).

[h] Samples were collected from the surfaces of river-polished, in-situ basalt of the West Crater lava flow.

[i] Duplicate analyses on the same sample material

[j] Sample probably contains inherited cosmogenic ^3He_c from previous exposure.

Geochemical Correlations of Owyhee River Lava Flows

The geochemical data alone do not conclusively distinguish the lava flows from each other because some of the flows are chemically heterogeneous, the data are sparse, and only single samples were analyzed from some flows. However, the patterns in the geochemical results support correlations drawn from other tools. For both major and trace elements, the samples from the Owyhee Butte and Bogus Rim lavas define the most geochemically distinct field (Figs. DR1a and DR1b). The West Crater and Rocky Butte/Clarks Butte fields are more chemically heterogeneous and overlap in some cases. The similar mineral assemblages of the West Crater, Rocky Butte, and Clarks Butte flows required the use of several other characteristics, such as relative stratigraphic and geomorphic position, relative soil development, and paleomagnetic signature, to identify and correlate isolated lava flow remnants.

Clarks Butte Lava Flow Geochemistry

Major and trace element data (Fig. DR1) produced from samples of the upper perched outcrops of lava at the AM-PM site (Rk 49) and at locations of similar outcrops downstream (Rk 65.25, 73.5, and 75.3; Fig. 2B) are consistent with the interpretation of these as isolated erosional remnants of the Clarks Butte lava flow. Geochemical analyses of samples OWY-35, OWY-37, OWY-21B, and OWY-21A, collected from these perched lavas, plot in a tight group in or near the Rocky Butte/Clarks Butte major element field and distinct from the West Crater field (Fig. DR1.a). These four samples are so chemically similar that they could represent a single, unique advance of a lava flow into the canyon. Although the samples taken near the source vents of the Clarks Butte and Rocky Butte lavas are geochemically similar, the Rocky Butte flow appears to have terminated before reaching the Owyhee Canyon and is even younger than the West Crater lava flow, inferred from differences in surface morphology, a poorly exposed contact relation, and a $^{40}K/^{39}Ar$ age of 30 ka (Hart and Mertzman, 1983). Sample OWY-21A, collected near RKm 75.25, marks the known downstream extent of the Clarks Butte flow, based on its affinity with the Rocky Butte/Clarks Butte major element field, high level of zirconium, and field relations with the other Clarks Butte lava remnants.

West Crater Lava Flow Geochemistry

Major element analyses from samples thought to be from the West Crater flow (samples OWY-22, OWY-23, OWY-31, and OWY-36) generally all plot within or near the West Crater field (Fig. DR 1.a). Two of these samples (OWY-22 and OWY-23) plot near or within the region of overlap between the Rocky Butte/Clarks Butte field and the West Crater field. However, the direction of remanent magnetization of sample 0348B collected at the same location as OWY-23 matches that of the West Crater lava flow (Table DR 2; for details of paleomagnetic analysis, see following section). Sample OWY-22 was collected higher in the stratigraphy than OWY-23 and therefore must be younger and not the Clarks Butte lava. Trace element analyses (Fig. DR1b) show sample OWY-23 commonly lies some distance from the West Crater field. However, analysis of the remanent magnetization of sample 0348B, collected from the same location as OWY-23, shows these outcrops to also be of West Crater affinity and supports the interpretation of these as early incursions of West Crater lava into the Owyhee Canyon.

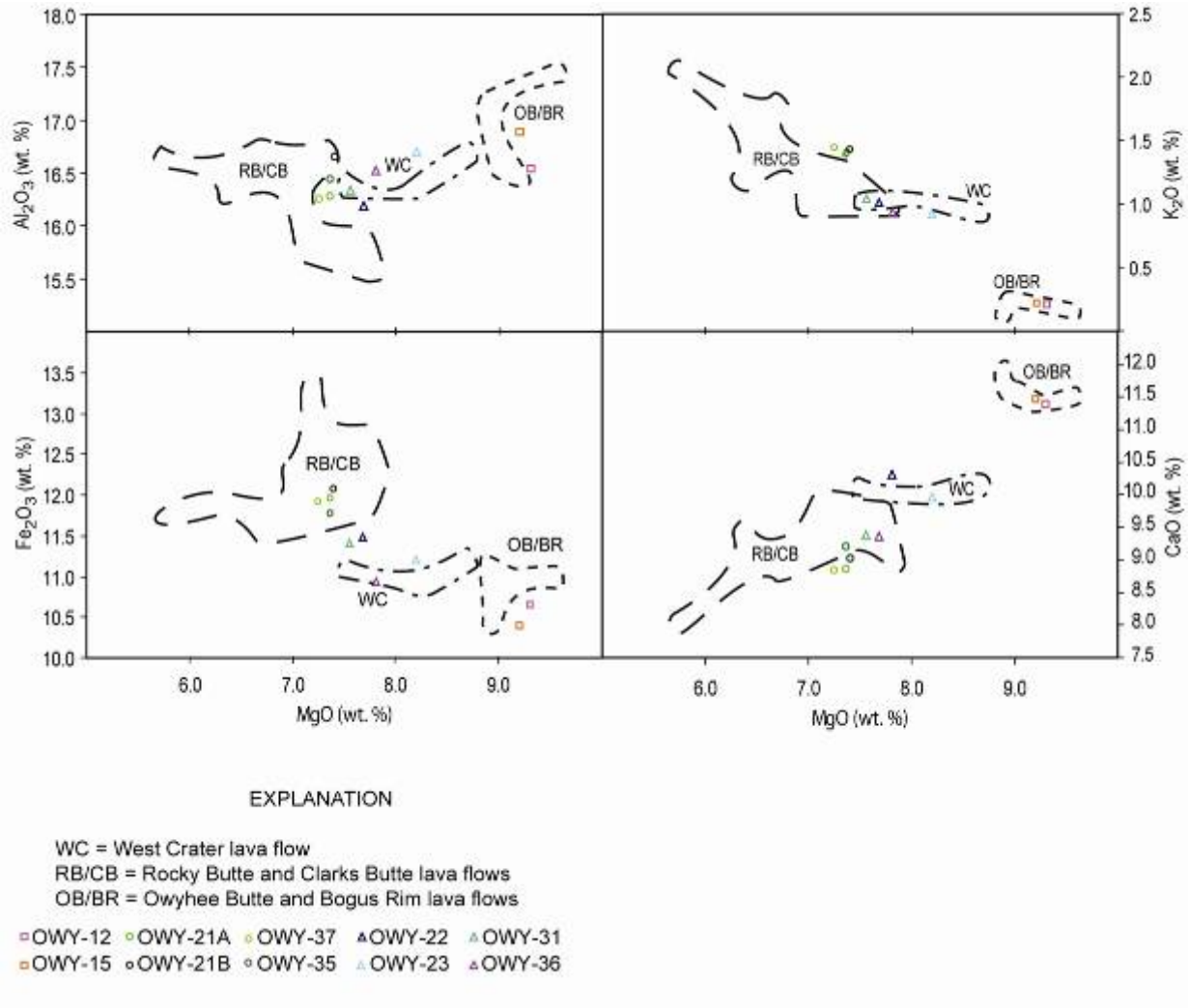

Figure DR 1a. Plots of major element analyses of select Owyhee lava flows: Al_2O_3 vs. MgO, Fe_2O_3 vs. MgO, K_2O vs. MgO, CaO vs. MgO. Dashed lines encompass the boundary of the fields representing the geochemical results for the following grouped lava flows, as defined by previous data tabulated in Bondre (2006): Rocky Butte (RB)/Clarks Butte (CB), Owyhee Butte (OB)/Bogus Rim (BR), and West Crater (WC). Individually plotted points represent new analyses of samples in this study, which were compared with the established geochemical fields (Bondre, 2006) to validate field correlations of isolated lava flows in the Owyhee River canyon to each other and their sources.

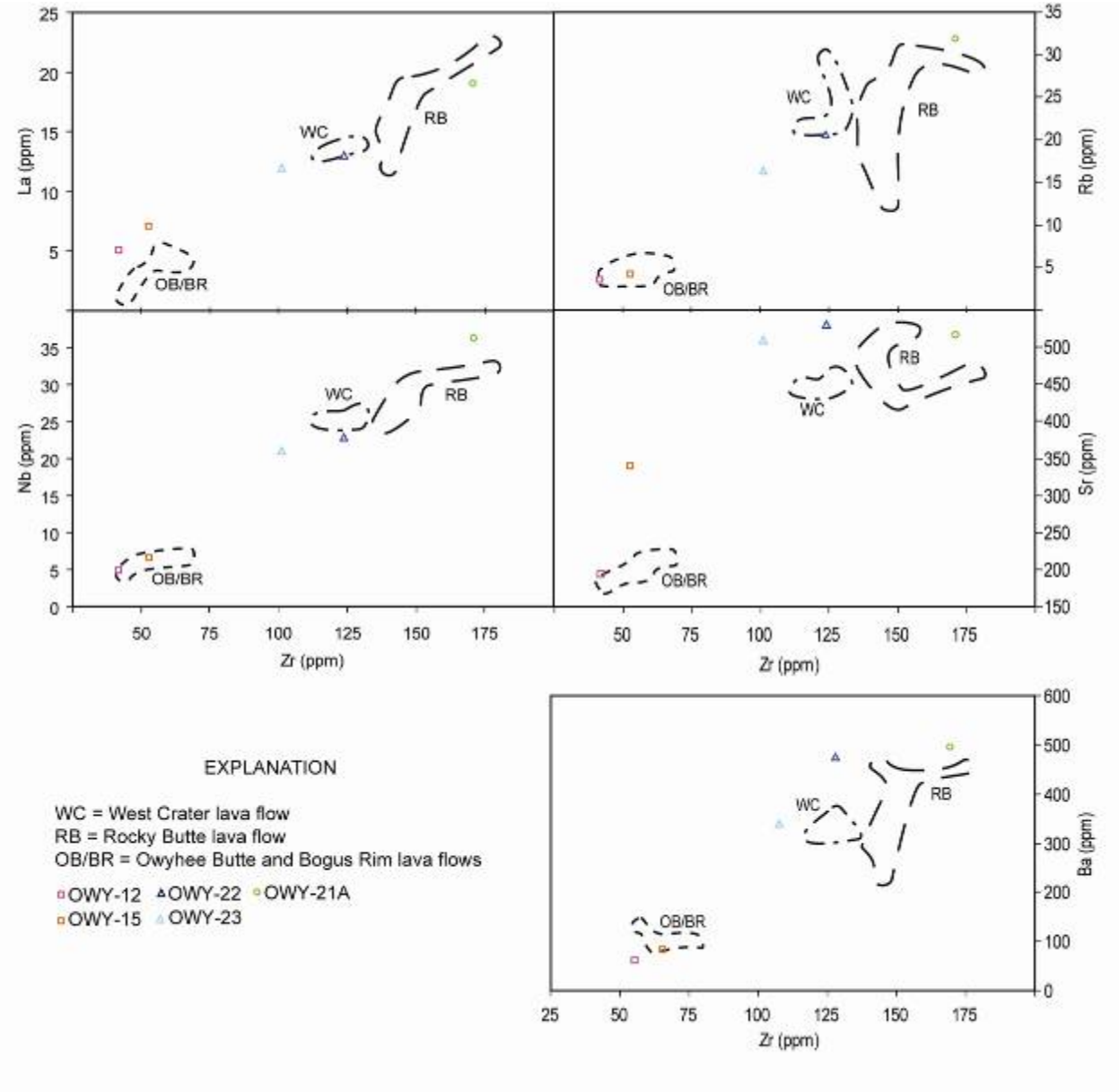

Figure DR 1b. Trace element analyses of select Owyhee lava flows: La vs. Zr, Nb vs. Zr, Rb vs. Zr, Sr vs. Zr, Ba vs. Zr. Descriptions of groupings and symbols are the same as in Fig. DR 1a.

Paleomagnetic Correlations of Owyhee River Lava Flows

Changes in the direction of remanent magnetization were used to distinguish among the lava flows found in the Owyhee Canyon and to correlate isolated lava outcrops to previously dated lava fields or vents flows (McElhinny, 1973; Kuntz et al., 1986; Butler, 1992; Champion and Shoemaker, 1977). Individual lava flows from known source vents were sampled to characterize the remanent magnetism and provide a base value to compare with isolated lava flow outcrops, following the methodology of Champion (1980). Paleomagnetic sample sites were occupied in outcrops from ten different lava fields (Table DR3). The sites were selected in horizontal, stable areas of the lava flows that had not been tilted after cooling and magnetization. Where possible, sample sites were located where the surface of the flow had been removed recently by erosion or in road cuts to reduce the presence of isothermal remanent magnetization (IRM) resulting from lightning strikes. A hand-held, water-cooled, gasoline-powered coring drill was used to collect eight independently oriented, 1-in diameter samples at each site. A sun compass was exclusively used to orient the azimuth of the field cores because the magnetic character of mafic volcanic rock influences a magnetic compass. The remanent magnetization of the cores was measured using an automatic cryogenic magnetometer at the US Geological Survey in Menlo Park, California. The mean directions of magnetization for each site were then calculated and plotted on an equal-area diagram (Fig. DR 2, Table DR 3).

Paleomagnetic techniques were more successful than geochemistry in distinguishing the lava flows from one another. All flows appear to have their own average directions of remanent magnetization (Fig. DR 2, Table DR 3). The scatter of remanent directions from these ten lava fields is representative both of the dispersion in directions due to geomagnetic secular variation through time, and of the precision of our field sampling protocol to capture these remanent directions. Among the flows with normal polarization, West Crater, Saddle Butte, and Forgotten Butte have average directions in fair proximity to one another. In the absence of any other information (appearance, position, stratigraphy, chemistry, etc.) individual sites in West Crater flows could be confused for Saddle Butte flows. But, as populations of sites, and informed by other sources of identification data, they can be differentiated. Among the four reversed polarity data sets (Fig. DR 2), individual sites from Deer Park outcrops could be confused with sites taken in Little Owyhee Butte lava flows. But, as they differ by a million years in age, and are spatially separated from one another, no such confusion occurs.

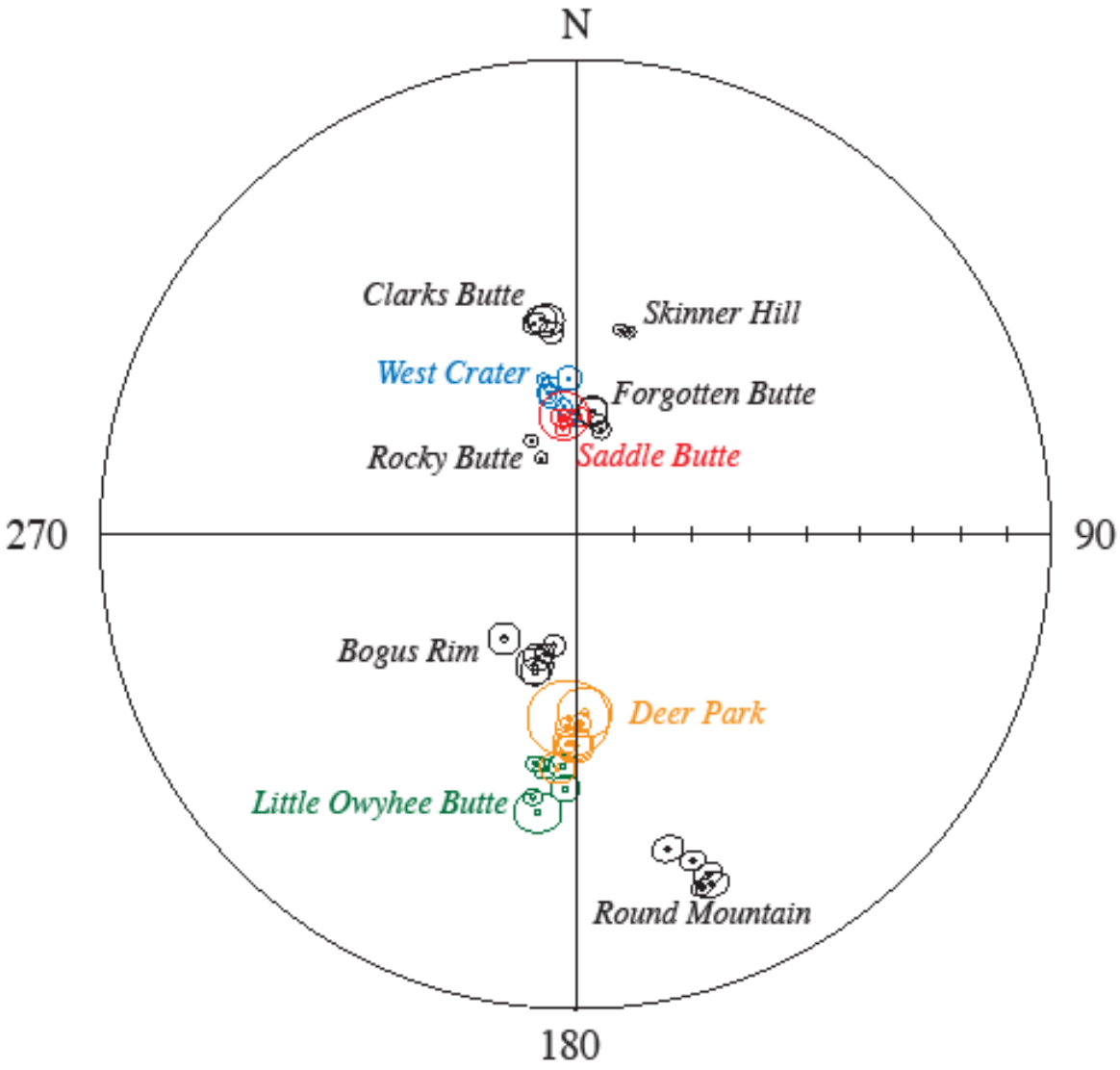

Figure DR 2. Equal-area diagram of mean directions of remanent magnetization with circles of 95% confidence for lava flows in this study. Samples were collected from lava outcrops near the source vents and within the Owyhee River canyon to validate correlations of isolated lava outcrops with each other and their sources. Directions of magnetization are depicted by the declination (east from true north) and the inclination (closed circles are positive and oriented downward, open circles are negative and oriented upward) from the horizontal (Butler, 1992; McElhinny, 1973). Samples with larger uncertainty were affected by lightning.

Table DR3. Middle Owyhee River and Jordan Valley Paleomagnetic Data

Unit Name	Site	Lat.*	Long.*	N/No	Exp.	I	D	α 95	k	R	Plat.	Plong.
West Crater lava field												
in Bogus Creek	650B6	43.084°	242.319°	8/8	20	65.3°	348.5°	1.6°	1184	7.99409	80.8°	184.6°
near Bogus Point	658B6	43.079°	242.322°	8/8	20	63.8°	350.5°	1.3°	1701	7.99589	82.8°	174.5°
on Airstrip Road	674B6	43.051°	242.389°	8/8	20	62.8°	348.2°	1.0°	3175	7.99780	81.4°	164.4°
50m W Bed Springs Gate	0178B	43.067°	242.317°	8/8	Mx	63.1°	357.5°	2.0°	856	7.9918	87.6°	193.2°
Bogus Falls-lowest flow unit	0348B	43.097°	242.293°	8/8	20+	65.9°	349.5°	1.9°	854	7.99180	81.1°	190.3°
SW of AM-PM Camp	0508B	43.134°	242.299°	8/8	40	70.5°	358.2°	1.0°	2851	7.99754	78.3°	237.1°
Lava Sinks Reservoir	9349B	43.017°	242.411°	8/8	30	68.0°	354.3°	1.3°	1813	7.99614	81.1°	218.7°
		43.08°	**242.34°**	**7/7**		**65.7°**	**352.2°**	**2.5°**	**604**	**6.99006**	**82.7°**	**196.3°**
Rocky Butte (Lava Butte) lava field												
N. side of canal	436B4	42.913°	242.594°	10/10	20	72.2°	334.5°	1.1°	1942	9.99537	68.5°	203.3°
Rocky Butte-S margin	1420B	42.940°	242.636°	8/8	Li	75.7°	335.7°	1.0°	3377	7.9979	65.5°	215.9°
		42.93°	**242.62°**	**2/2**		**74.0°**	**335.0°**	**7.7°**	**1063**	**1.99906**	**67.1°**	**209.8°**
Saddle Butte lava field												
on Hwy 78	428B4	42.957°	241.951°	7/8	20	71.8°	353.0°	1.3°	2016	6.99702	75.6°	226.3°
near BM 3681-Tub Springs Rd	682B6	42.982°	242.253°	8/8	20	69.8°	352.4°	1.5°	1314	7.99467	78.2°	219.7°
Ryegrass Creek	690B6	43.038°	242.260°	8/8	Pl	69.6°	354.3°	4.1°	227	----	79.0°	224.1°
S*and Springs Camp-lower*	18B	43.009°	242.269°	8/8	20+	(67.5°	6.4°)	1.6°	1181	7.99407	81.5°	270.9°
@river km-38.75	*0098B*	*43.067°*	*242.304°*	*8/8*	*20+*	*(61.3°*	*344.1°)*	*1.4°*	*1560*	*7.99551*	*78.3°*	*154.6°*
paleochannel of Ryegrass	0258B	43.071°	242.306°	9/9	20+	69.9°	2.2°	1.6°	1007	8.99206	79.2°	249.1°
Saddle Butte near Sand Springs	3580B	43.009°	242.270°	8/8	Li	70.0°	355.8°	1.5°	1385	7.9949	78.7°	229.5°
		43.01°	**242.1°**	**5/7**		**70.3°**	**355.6°**	**1.5°**	**2531**	**4.99842**	**78.3°**	**229.3°**
Skinner Hill lava field												
on road to Danner	446B4	42.955°	242.742°	7/8	30+	53.7°	12.2°	1.0°	3668	6.99836	77.1°	11.3°
E side near Jordan Crater	462B7	42.990°	242.793°	7/8	20	53.7°	14.8°	1.0°	3751	6.99840	75.6°	5.0°
		42.97°	**242.77°**	**2.2**		**53.7°**	**13.5°**	**3.4°**	**5544**	**1.99982**	**76.3°**	**8.0°**
Forgotten Butte (vent 4526')												
W. "rootless" vent	706B6	43.070°	242.484°	8/8	20	71.6°	13.7°	1.5°	1411	7.99504	74.1°	271.1°
N. of Bogus Lake	8949B	43.057°	242.426°	7/8	40	68.8°	7.8°	2.4°	654	6.99082	79.5°	269.7°
N side, W of contact	9109B	43.078°	242.531°	7/8	40	70.6°	11.6°	1.5°	1548	6.99612	76.0°	271.1°
W of Rocky Butte	9189B	43.023°	242.465°	7/8	40	68.5°	7.8°	2.4°	643	6.99067	79.8°	270.8°
		43.06°	**242.48°**	**4/4**		**69.9°**	**10.1°**	**2.0°**	**2065**	**3.99855**	**77.4°**	**270.7°**

Clarks Butte lava field												
Clarks Butte – E. side	470B7	43.043°	242.645°	7/8	Pl	54.7°	353.1°	1.9°	1282	6.9953	80.5°	99.3°
SW of AM-PM Camp	0428B	43.134°	242.292°	8/8	20+	52.6°	348.9°	1.9°	838	7.99165	76.8°	107.1°
AM-PM Hole-in-the-ground	0588B	43.209°	242.407°	8/8	30+	52.5°	352.2°	2.8°	352	7.98203	78.2°	96.3°
upstream of Birch Creek	0668B	43.214°	242.486°	8/8	40	52.2°	351.0°	2.4°	535	7.98692	77.4°	99.7°
N side, E of contact	*9029B*	*43.076°*	*242.544°*	*4/8*	*Mx*	*(56.4°*	*4.6°)*	*4.1°*	*940*	*3.9968*	*83.0°*	*31.1°*
		43.15°	**242.46°**	**4/5**		**53.0°**	**351.3°**	**1.8°**	**2626**	**3.99886**	**78.3°**	**100.8°**
Greeley Bar area												
outcrop on bench – top flow?	429B7	43.198°	242.452°	9/9	Li	-57.3°	178.6°	1.6°	1053	8.9924	-84.6°	254.3°
@ base of lava cascade	438B7	43.191°	242.457°	8/8	40	-56.4°	183.0°	1.6°	1190	7.99412	-83.4°	221.4°
ridge leading from 4621’	446B7	43.161°	242.487°	8/8	Pl	-58.0°	182.4°	6.7°	-----	-----	-85.2°	219.8°
top of Sect. 7	1979B	43.145°	242.494°	7/8	Mx	-59.1°	177.1°	4.4°	253	6.9763	-86.1°	277.1°
NW corner Sect. 18	2059B	43.132°	242.481°	8/8	Mx	-53.5°	182.1°	1.5°	1523	7.9954	-80.8°	231.6°
basalt of Greeley Bar-far W	0860B	43.174°	242.448°	5/8	Li	-49.1°	184.4°	2.8°	778	4.9949	-76.4°	226.1°
		43.17°	**242.47°**	**6/6**		**-55.6°**	**181.4°**	**3.3°**	**408**	**5.98774**	**-82.9°**	**233.2°**
Deer Park vent												
NW shoulder vent 4737’	2139B	43.175	242.485°	8/8	Mx	-53.2°	180.3°	3.0°	351	7.9800	-80.6°	241.0°
upper Deer Park cascade	2219B	43.174°	242.481°	8/8	Mx	-53.7°	181.0°	3.1°	354	7.9802	-81.0°	237.2°
		43.175°	**242.483°**	**2/2**		**-53.5°**	**180.7°**	**1.4°**	**31069**	**1.99997**	**-80.8°**	**239.1°**
Round Mountain												
Hwy 93 road cut	2379B	42.849°	242.389°	8/8	Mx	-27.8°	160.3°	1.9°	860	7.9919	-57.2°	279.4°
Round Mountain – NW side	2060B	42.812°	242.400°	8/8	Li	-22.0°	160.4°	1.5°	1450	7.9952	-54.3°	276.7°
Round Mountain – SW side	2140B	42.796°	242.426°	7/8	Li	-24.2°	158.7°	2.1°	836	6.9928	-54.7°	280.2°
Round Mountain – SE side	2220B	42.787°	242.498°	7/8	Mx	-31.5°	163.7°	2.4°	615	6.9902	-60.8°	275.8°
S. of Jordan Ck–Round Mtn	4060B	42.862°	242.379°	8/8	Mx	-21.7°	158.8°	2.4°	559	7.9875	-53.4°	278.9°
		43.82°	**242.42°**	**5/5**		**-25.5°**	**160.3°**	**4.3°**	**318**	**4.98743**	**-55.2°**	**277.4°**
Little Owyhee Butte												
road up from bridge	2459B	42.879°	242.355°	8/8	Mx	-40.5°	187.8°	3.7°	232	7.9698	-69.2°	221.8°
S. of Pascuale Reservoir	2539B	42.902°	242.386°	8/8	40	-48.6°	187.6°	1.7°	1017	7.99312	-75.4°	215.2°
S central Sect. 33	2859B	42.906°	242.305°	7/8	40	-49.4°	190.0°	1.4°	1911	6.99686	-75.0°	206.7°
SW corner Hidden Valley	3259B	42.921°	242.431°	8/8	40	-45.4°	182.4°	2.3°	566	7.98762	-73.9°	234.8°
Above “gooseneck”	3339B	42.889°	242.414°	7/8	Mx	-49.5°	183.2°	2.2°	1039	6.9942	-77.2°	229.9°
Little Owyhee B.-satellite vent	4140B	42.921°	242.332°	8/8	Mx	-43.2°	189.3°	1.4°	1720	7.9959	-70.7°	216.1°
		42.90°	**242.37°**	**6/6**		**-46.1°**	**186.7°**	**3.6°**	**354**	**5.98587**	**-73.6°**	**220.7°**

Bogus Rim lava flow												
near Bogus Falls	698B6	43.048°	242.397°	8/8	Pl	-68.2°	214.5°	2.7°	707	----	-65.4°	120.6°
N side Bogus Bench	2299B	43.090°	242.451°	8/8	Mx	-65.3°	196.6°	2.3°	641	7.9891	-77.6°	126.5°
White Wash Reser.	8789B	43.077°	242.342°	8/8	Mx	-70.5°	191.1°	1.8°	1016	7.9931	-76.3°	90.4°
Dry Creek Reservoir	8869B	43.107°	242.314°	8/8	40	-67.8°	197.3°	2.3°	580	7.98793	-76.0°	113.1°
rim flow-Rinehart Ranch	9509B	43.206°	242.367°	8/8	Li	-68.8°	194.3°	1.5°	1340	7.9948	-76.9°	104.2°
1st Castle-Birch Creek Ranch	0940B	43.216°	242.494°	8/8	Mx	-66.2°	197.5°	3.1°	317	7.9779	-76.7°	122.6°
		43.1°	**242.39°**	**6/6**		**-68.0°**	**198.6°**	**2.9°**	**521**	**5.99040**	**-75.1°**	**113.8°**

* NAD 27 datum was used for the decimal degree coordinates of the paleomagnetic sample sites. Longitude values are 360-degree coordinates.

Table DR4. Representative Sample Descriptions of Select Owyhee River Lava Units

Bogus Point Lava
A light gray to gray unit, with a fine-grained groundmass of dark grey and white crystals < 0.75 mm in diameter. Rare ~1.5 mm euhedral pale green olivine phenocrysts make up < 1% of the rock; orange secondary crystals < 0.5 mm where weathered.

Bogus Rim Lava
A gray, fine-grained unit with a felty texture having few subhedral to anhedral phenocrysts of plagioclase. Plagioclase phenocrysts 0.3–0.5 mm in length make up ~1-3% of the rock. Olivine phenocrysts also comprise ~1-3% of the rock and are light pale green, commonly < 0.5 mm, and rarely ~1 mm in diameter.

Deer Park Lava
Composed of two petrologically different sub units: a plagioclase phyric diktytaxitic textured flow unit (south and west of hill 4737, including unnamed lava cascade) and a dense olivine phyric flow unit (north side of hill 4737 and Deer Park lava cascade).

A fine grained, darker gray, plagioclase olivine phyric diktytaxitic unit. Plagioclase laths and needles range from 1-6 mm long, commonly are 3-4 mm. Light green, to olive, to yellow-olive, and occasional orange olivine phenocrysts are 1-3 mm, olivine glomerocrysts are common. Some metallic orange-purple (pyroxene?) crystals are < 0.5 mm.

A fine grained, lighter gray, olivine phyric, dense unit exhibiting weak if any diktytaxitic texture. Olivine phenocrysts are lime green to olive to yellow green and rarely brown, 1-2 mm occur sometimes as 2-4 mm glomerocrysts. Rock is lacking plagioclase phenocrysts but has fine-grained ground mass of <0.25 mm plagioclase, < 0.25 mm dull dark purple hematite crystals, and < 1 mm pyroxene crystals.

Clarks Butte Lava
A dark gray, fine-grained unit. Some samples contain vesicles that are partly to completely filled with white and tan secondary minerals. Plagioclase phenocrysts generally constitute < 3-5% of the rock, but occasionally > 10%. Most are subhedral to euhedral crystals < 0.5-1 mm in diameter, but occasionally as 1–3 mm laths or plates that show good cleavage. Subhedral olivine phenocrysts range from pale green to reddish brown in color and are usually < 1 mm in diameter, but occasional 2 mm phenocrysts occur. Olivine phenocrysts generally compose ~5–15%, but sometimes as much as 20-30%, of the rock.

Saddle Butte Lava
A medium gray, fine-grained unit. White phenocrysts < 0.5 mm in diameter are common. Small, pale green to olive-colored subhedral olivine phenocrysts 0.25-0.5 mm in diameter are fairly common; olivine phenocrysts > 1 mm are rare (<1% of the rock). Occasional bright green phenocrysts of olivine are 1.5–2 mm in diameter.

West Crater Lava
A medium gray to dark gray, fine-grained unit exhibiting a diktytaxitic texture with abundant fresh phenocrysts of olivine and plagioclase and slightly altered olivine. Olivine occurs as brilliant pale green to olive to brown anhedral crystals up to 6 mm but more commonly < 4 mm in diameter. Plagioclase phenocrysts comprise 15–35% of the rock while olivine phenocrysts constitute < 10-20%. Euhedral plagioclase laths show twinning and range up to 1 by 10 mm in size, though are more commonly ~0.5 by 3–4 mm. Anhedral to subhedral tabular plagioclase crystals are up to 4 by 5 mm in size, though more commonly are 2 by 3 mm and sometimes show striations. Orange and tan secondary minerals occupy space in vesicles and tiny black prismatic crystals cluster around and project into vesicles.

Saddle Butte Lava Flow $^{40}Ar/^{39}Ar$ Analytical Results

Sample 428B4 from the Saddle Butte lava flow was analyzed by Brent Turrin at Rutgers University. The sample preparation and analysis followed the procedures for $^{40}Ar/^{39}Ar$ dating of young basalts in Turrin et al. (2008). The resulting analytical uncertainty on this sample was particularly low, 144 ± 14 ka. To determine and track any potential changes in mass spectrometer mass discrimination during the course of the step-heating experiment, ~7 $\times 10^{-14}$ moles of atmospheric argon were pipetted into the extraction/mass spectrometer system approximately every 1.5 to 2 hours to monitor any changes in the mass spectrometer mass discrimination. To minimize possible dependence of mass discrimination on beam current, we attempted to keep the beam intensity of each step in the sample-extraction experiments within a factor of two of the beam intensity during measurement of the mass discrimination air pipettes.

The neutron fluence parameter, "J," for the sample irradiation was determined using an age of 1.194 ± 0.006 Ma for sanidine from the rhyolite of Alder Creek, California (Renne et al., 1998). Interfering neutron reactions from Ca and K (Brereton, 1970; Dalrymple et al., 1981) were corrected by using the following values $(^{36}Ar/^{37}Ar)_{Ca} = (2.72 \pm 0.06) \times 10^{-4}$; $(^{39}Ar/^{37}Ar)_{Ca} = (7.11 \pm 0.02) \times 10^{-4}$ (Renne et al., 1998; Deino and McBrearty, 2002). Age calculations were made using the current accepted decay constants and isotopic abundances (Steiger and Jager, 1977): $\lambda\varepsilon = 5.81 \times 10^{-11}$ yr^{-1}, $\lambda\beta = 4.962 \times 10^{-10}$ yr^{-1}, $^{40}K/K = 1.167 \times 10^{-4}$.The plateau ages and their pooled errors were calculated following Dalrymple and Lanphere (1974), using the variance-weighted mean of the plateau steps.

Table DR 5. $^{40}Ar/^{39}Ar$ Analytical Results from Saddle Butte lava flow sample 428B4 (analyzed by B. Turrin, Rutgers University).

Run ID		Watts	Ca/K	$^{36}Ar/^{39}Ar$	$\%^{36}Ar_{Ca}$	$^{40}Ar^*/^{39}Ar$	Moles ^{39}Ar x10^{-16}	$^{39}Ar_K$ % Step	$^{39}Ar_K$ Cum%	$\%^{40}Ar^*$	Age (ka)	±1 σ
Saddle Butte, Run ID# 20334-01												
20334-01A		*1*	29.8412	0.30845	1.3	4.6401	2.4107	5.6	5.6	4.9	385	95
20334-01B		*2*	35.4978	0.18119	2.7	0.6043	7.4656	12.8	18.4	1.1	50	54
20334-01C		4	22.2144	0.10215	3	1.2364	3.1852	7.4	25.8	4	102	34
20334-01D		6	12.7957	0.12028	1.5	2.2034	8.8496	20.6	46.3	5.9	183	31
20334-01E		8	11.8175	0.16854	1	1.7574	6.2335	14.5	60.8	3.4	146	31
20334-01F		10	14.6663	0.27423	0.7	1.9924	4.1897	9.7	70.5	2.4	165	32
20334-01G		12	22.3292	0.36136	0.9	1.3326	3.5601	8.3	78.8	1.2	110	45
20334-01H		14	33.4304	0.43149	1.1	1.2007	2.5462	5.9	84.7	0.9	100	64
20334-01I		17	53.6776	0.62567	1.2	1.1832	2.5640	6	90.7	0.6	98	84
20334-01J		20	74.7207	0.68185	1.5	2.7650	1.6257	3.8	94.4	1.3	229	105
20334-01K		*25*	75.1950	0.75668	1.4	5.3163	*1.4840*	3.4	97.9	2.3	441	117
20334-01L		*30*	61.7071	0.80848	1.1	2.4880	*9.1343*	2.1	100	1	206	221
J = 0.0000459 ± 4.060000e-7												

Sample Summary											
	Material		**Integ Age (ka)**	**±1σ**	**Plat age (ka)**	**±1 σ**	**MSWD**	**Prob**	**Steps**	**N/N-total**	**%Gas**	
	wr/ matrix		160	30	144	14	0.8	0.6	C-J	8/11	76.1	
	Iso all plat	**±1 σ**	**$^{40}Ar/^{36}Ar$ (init)**	**±1 σ**	**MSWD**	**N**	**Iso all points**	**±1□**	**40Ar/36Ar (init)**	**±1s**	**MSWD**	**N**
	150	20	295.2	1.2	0.9	8	120	30	296.9	1.5	1.5	12

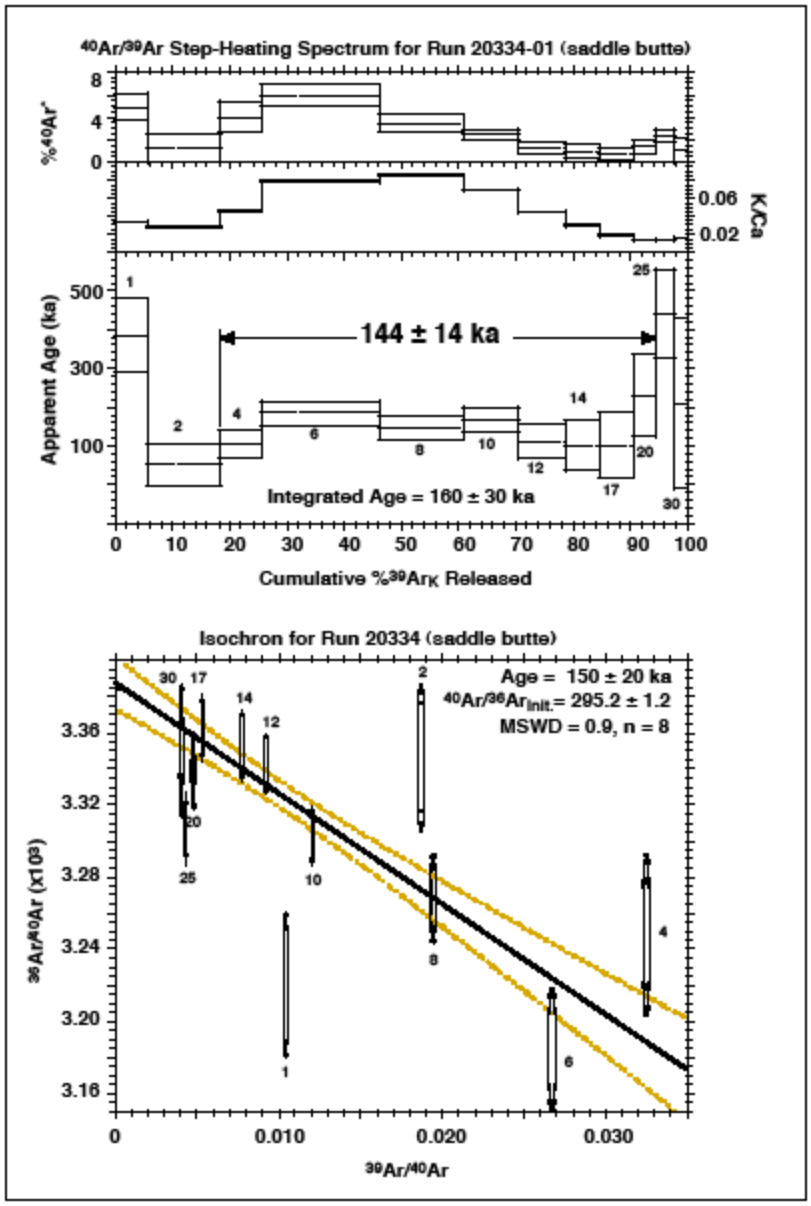

Figure DR 3. Plateau and isochron results from the $^{40}Ar/^{39}Ar$ experiment on Saddle Butte lava flow sample 428B4, Brent Turrin, Rutgers University.

$^{40}Ar/^{39}Ar$ Analytical Results of Samples Processed at New Mexico Geochronology Research Laboratory

Samples analyzed at the New Mexico Geochronology Research Laboratory at the New Mexico Institute of Mining and Geology were prepared by coarse crushing and sieving to 60-80 mesh. Olivine, which can have excess Ar, was removed by magnetic separation and laborious hand picking. Samples were leached with dilute HCl to remove calcite, although calcite does not appear to have been present in any sample, then rinsed repeatedly with distilled H_2O. Samples were irradiated for 1 hour at the Triga reactor of the U.S. Geological Survey, Denver. Samples were heated at progressively higher power with a CO_2 laser and broad beam. Released gases were analyzed on a MAP 215-50 mass spectrometer using methods detailed in McIntosh et al. (2003). Lines with X in the first column in the Data Repository are not used in the plateau age calculated for that sample. All ages are calculated using Fish Canyon sanidine at 28.02 Ma (Renne et al., 1998).

The youngest and oldest samples (0428B and 9429B) give straightforward results, with flat spectra and inverse isochron and total gas ages that agree closely with plateau ages. The other two samples have irregular spectra, and neither gives an unequivocal age. The spectrum for sample 429B7 climbs fairly continuously, although the D step has an anomalously young age and extremely low radiogenic content. Eliminating the D step with the assumption that it has some unknown but significant error, the B, C, E, F, and G steps give an apparent age of 0.78±0.10 Ma, which agrees with the inverse isochron age of 0.7±0.2 Ma. The flow is probably about 0.7 to 0.8 Ma.

The spectrum for sample 3419B also climbs continuously. All steps have low radiogenic yields, ≤8%, which makes calculations highly sensitive to blanks and measured ^{36}Ar concentrations. Contiguous steps D, F, and K make a plateau of 1.01±0.28 Ma, which is indistinguishable from the total gas age. The inverse isochron age is highly imprecise because of the low radiogenic yields. The best age estimate is about 1 Ma, but with considerable uncertainty.

Table DR 6a. Summary of $^{40}Ar/^{39}Ar$ Analytical Results, New Mexico Geochronology Research Laboratory

*Ages reported to ±2 sigma were converted to ± 1 sigma for Table DR 1 and weighted mean calculations.

Sample[1]	Lava Flow	Ages (Ma)[2]										
		plateau	±2s	$\%^{39}Ar$[3]	steps	isochron	±2s[4]	$^{40}Ar/^{36}Ari$	±2s	MSWD	total gas	±2s
0428B	Clarks Butte	**0.220**	0.020	94.5	8/9	0.20	0.04	302	12	2.6	0.23	0.02
429B7	Deer Park	**0.78**	0.10	56.3	5/10	0.7	0.2	300	20	29	0.68	0.06
3419B	Bogus flow group, Bogus Point	1.01	0.28	65.7	3/9	0.6	0.4	301	12	17	0.99	0.21
9429B	uppermost unit of lower Bogus flows	**1.672**	0.059	98.0	9/10	1.69	0.12	292	13	2.7	1.67	0.07

[1] Analyses at the New Mexico Geochronology Research Laboratory (methodology in McIntosh et al., 2003). Neutron flux monitor Fish Canyon Tuff sanidine (FC-1). Assigned age = 28.02 Ma (Renne et al., 1998). Decay constants and isotopic abundances after Steiger and Jäger (1977); $l_b = 4.963 \times 10^{-10}$ yr^{-1}; $l_{e+e'} = 0.581 \times 10^{-10}$ yr^{-1}; $^{40}K/K = 1.167 \times 10^{-4}$

[2] Ages in bold are best estimates of eruption age. See text for discussion.

[3] $\%^{39}Ar$ = percentage of ^{39}Ar used to define plateau age.

[4] Ages reported to ±2 sigma were converted to ± 1 sigma for Table DR 1 and weighted mean calculations.

Table DR 6b. $^{40}Ar/^{39}Ar$ Analytical Results, New Mexico Geochronology Research Laboratory.

*Ages reported to ±2 sigma were converted to ± 1 sigma for Table DR 1 and weighted mean calculations.

	ID	Power	$^{40}Ar/^{39}Ar$	$^{37}Ar/^{39}Ar$	$^{36}Ar/^{39}Ar$	$^{39}Ar_K$	K/Ca	$^{40}Ar^*$	^{39}Ar	Age	±1s
		(Watts)			(x 10^{-3})	(x 10^{-15} mol)		(%)	(%)	(Ma)	(Ma)
	0428B, Clarks Butte lava flow, WR, 45 mg, J=0.0002489±0.11%, D=1.006±0.001, NM-229J, Lab#=59435-01										
	K	2	10.75	3.312	36.09	1.68	0.15	3.3	4.3	0.158	0.064
	M	3	1.773	1.409	4.901	5.65	0.36	24.5	18.7	0.194	0.013
	N	4	2.031	1.187	5.616	8.15	0.43	22.8	39.5	0.207	0.012
	O	5	2.314	0.8979	6.393	5.83	0.57	21.3	54.3	0.220	0.014
	P	8	3.029	1.100	8.537	6.46	0.46	19.5	70.8	0.264	0.016
	Q	13	4.301	2.017	13.27	5.40	0.25	12.5	84.5	0.241	0.022
	R	16	4.440	2.630	13.67	2.45	0.19	13.8	90.7	0.274	0.041
	S	18	4.800	3.382	14.93	1.48	0.15	13.7	94.5	0.296	0.052
X	T	30	7.332	10.48	26.05	2.15	0.049	6.7	100.0	0.223	0.057
	Integrated age ± 2s			n=9		39.3	0.25		K2O=1.35%	0.227	0.021
	Plateau ± 2s	steps K-S		n=8	MSWD=2.63	37.1	0.38 ±0.31		94.5	0.220	0.020

	ID	Power	$^{40}Ar/^{39}Ar$	$^{37}Ar/^{39}Ar$	$^{36}Ar/^{39}Ar$	$^{39}Ar_K$	K/Ca	$^{40}Ar^*$	^{39}Ar	Age	±1s
	429B7, Deer Park lava flow, WR, 53 mg, J=0.0002483±0.14%, D=1.006±0.001, NM-229J, Lab#=59436-01										
X	A	3	16.60	-0.7026	53.41	3.90	-	4.5	22.8	0.335	0.063
	B	4	4.499	4.432	10.85	4.19	0.12	36.7	47.4	0.741	0.025
	C	5	4.411	3.378	10.18	2.18	0.15	38.0	60.1	0.751	0.037
X	D	6	6.031	-16.7755	15.42	2.25	-	1.3	73.3	0.035	0.076
	E	8	10.78	4.848	29.97	1.45	0.11	21.5	81.8	1.038	0.069
	F	10	14.60	6.674	43.85	0.866	0.076	15.0	86.9	0.98	0.11
	G	13	19.84	11.00	62.32	0.931	0.046	11.7	92.4	1.05	0.11
X	H	16	24.98	16.23	76.66	0.620	0.031	14.7	96.0	1.66	0.16
X	I	18	26.91	17.90	84.18	0.310	0.028	13.0	97.8	1.59	0.26
X	J	30	43.11	50.74	149.8	0.374	0.010	7.0	100.0	1.41	0.33
	Integrated age ± 2s			n=10		17.1	0.20		K2O=0.50%	0.675	0.058
	Plateau ± 2s	steps B-G		n=5	MSWD=6.67	9.613	0.112±0.079		56.3	0.78	0.100
	3419B, Lower Bogus flow at Bogus Point, WR, 90 mg, J=0.0002494±0.10%, D=1.006±0.001, NM-229J, Lab#=59434-01										
X	A	2	178.5	23.68	615.2	0.625	0.022	-0.8	4.3	-0.63	0.57
X	B	3	58.40	18.42	199.6	0.898	0.028	1.6	10.4	0.43	0.22
X	C	3	35.75	-3.1694	119.4	1.31	-	0.6	19.3	0.09	0.17
	D	4	23.38	5.044	74.29	2.92	0.10	7.8	39.3	0.827	0.081
	F	8	37.76	6.149	121.1	4.24	0.083	6.5	68.2	1.112	0.094
	K	13	57.10	8.005	185.4	2.46	0.064	5.2	85.0	1.34	0.14
X	L	16	89.64	11.75	286.9	0.877	0.043	6.5	91.0	2.64	0.27
X	M	18	121.7	14.64	390.9	0.409	0.035	6.0	93.8	3.34	0.43
X	N	30	63.77	1.869	214.6	0.906	0.27	0.8	100.0	0.23	0.25
	Integrated age ± 2s			n=9		14.6	0.070		K2O=0.25%	0.99	0.21
	Plateau ± 2s	steps D-K		n=3	MSWD=6.14	9.621	0.084±0.037		65.7	1.01	0.277
	9429B, uppermost lower Bogus lava flow, WR, 52 mg, J=0.0002494±0.10%, D=1.006±0.001, NM-229J, Lab#=59433-01										
	A	3	12.52	7.064	32.17	3.81	0.072	28.7	25.3	1.623	0.042
	B	4	6.858	7.350	13.03	3.47	0.069	52.7	48.2	1.630	0.037
	C	5	7.117	6.474	12.47	1.78	0.079	55.7	60.1	1.788	0.045
	D	6	8.460	6.325	18.41	2.05	0.081	41.8	73.6	1.596	0.049
	E	8	9.905	6.572	22.02	1.31	0.078	39.8	82.4	1.777	0.065

	F	10	12.78	7.260	32.77	0.845	0.070	28.9	88.0	1.665	0.098
	G	13	16.50	9.990	45.79	0.777	0.051	23.0	93.1	1.72	0.12
	ID	**Power**	**$^{40}Ar/^{39}Ar$**	**$^{37}Ar/^{39}Ar$**	**$^{36}Ar/^{39}Ar$**	**$^{39}Ar_K$**	**K/Ca**	**$^{40}Ar^*$**	**^{39}Ar**	**Age**	**±1s**
	H	16	21.17	13.34	63.48	0.490	0.038	16.6	96.3	1.59	0.17
	I	18	23.79	18.07	68.81	0.253	0.028	20.8	98.0	2.25	0.29
Xi	J	30	35.55	47.16	122.0	0.298	0.011	9.5	100.0	1.58	0.39
	Integrated age ± 2s			n=10		15.1	0.062		K2O=0.45%	1.670	0.066
	Plateau ± 2s		steps A-I	n=9	MSWD=2.33	14.8	0.071±0.038		98.0	1.672	0.059

Notes:

Isotopic ratios corrected for blank, radioactive decay, and mass discrimination, not corrected for interfering reactions.
Errors quoted for individual analyses include analytical error only, without interfering reaction or J uncertainties.
Integrated age calculated by summing isotopic measurements of all steps.
Integrated age error calculated by quadratically combining errors of isotopic measurements of all steps.
Plateau age is inverse-variance-weighted mean of selected steps.
Plateau age error is inverse-variance-weighted mean error (Taylor, 1997) times root MSWD where MSWD>1.
Plateau error is weighted error of Taylor (1997).
Decay constants and isotopic abundances after Steiger and Jäger (1977).
symbol preceding sample ID denotes analyses excluded from plateau age calculations.
Weight percent K2O calculated from 39Ar signal, sample weight, and instrument sensitivity.
Ages calculated relative to FC-2 Fish Canyon Tuff sanidine interlaboratory standard at 28.02 Ma
Decay Constant (LambdaK (total)) = 5.543e-10/a
Correction factors:
($^{39}Ar/^{37}Ar$)Ca = 0.0007 ± 5e-05
($^{36}Ar/^{37}Ar$)Ca = 0.00028 ± 2e-05
($^{38}Ar/^{39}Ar$)K = 0.013
($^{40}Ar/^{39}Ar$)K = 0.01 ± 0.002

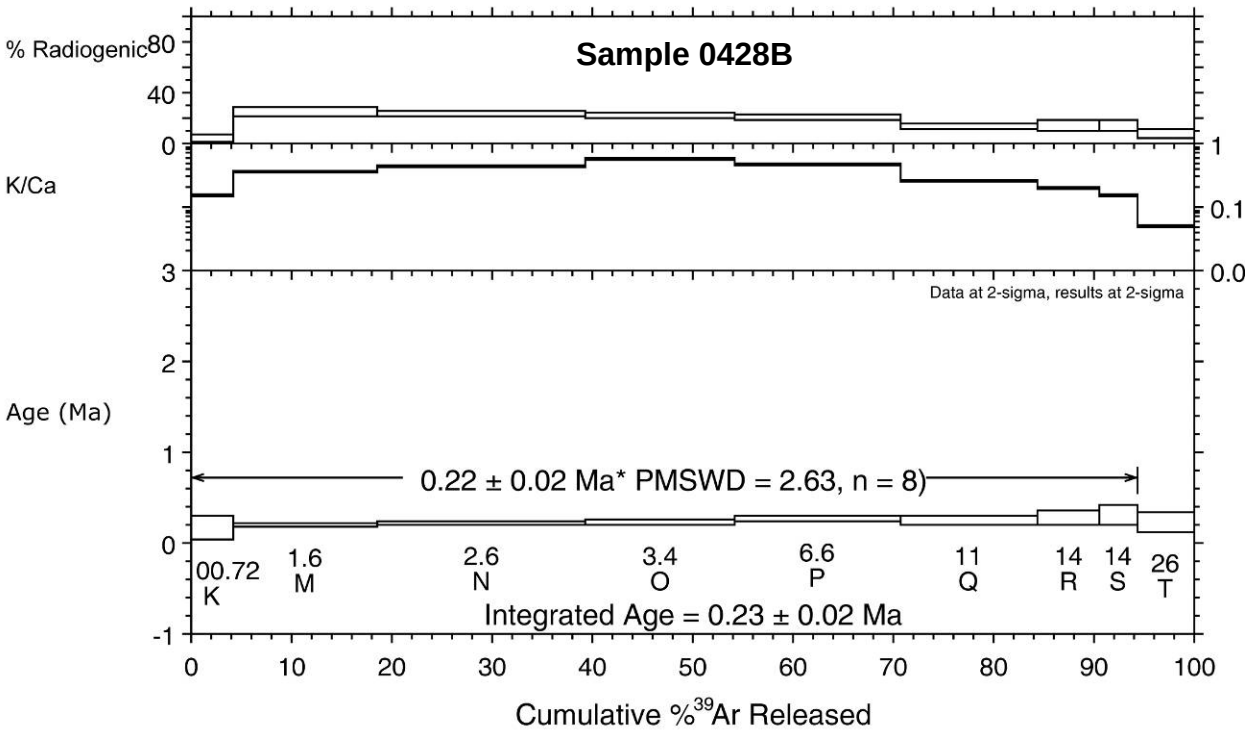

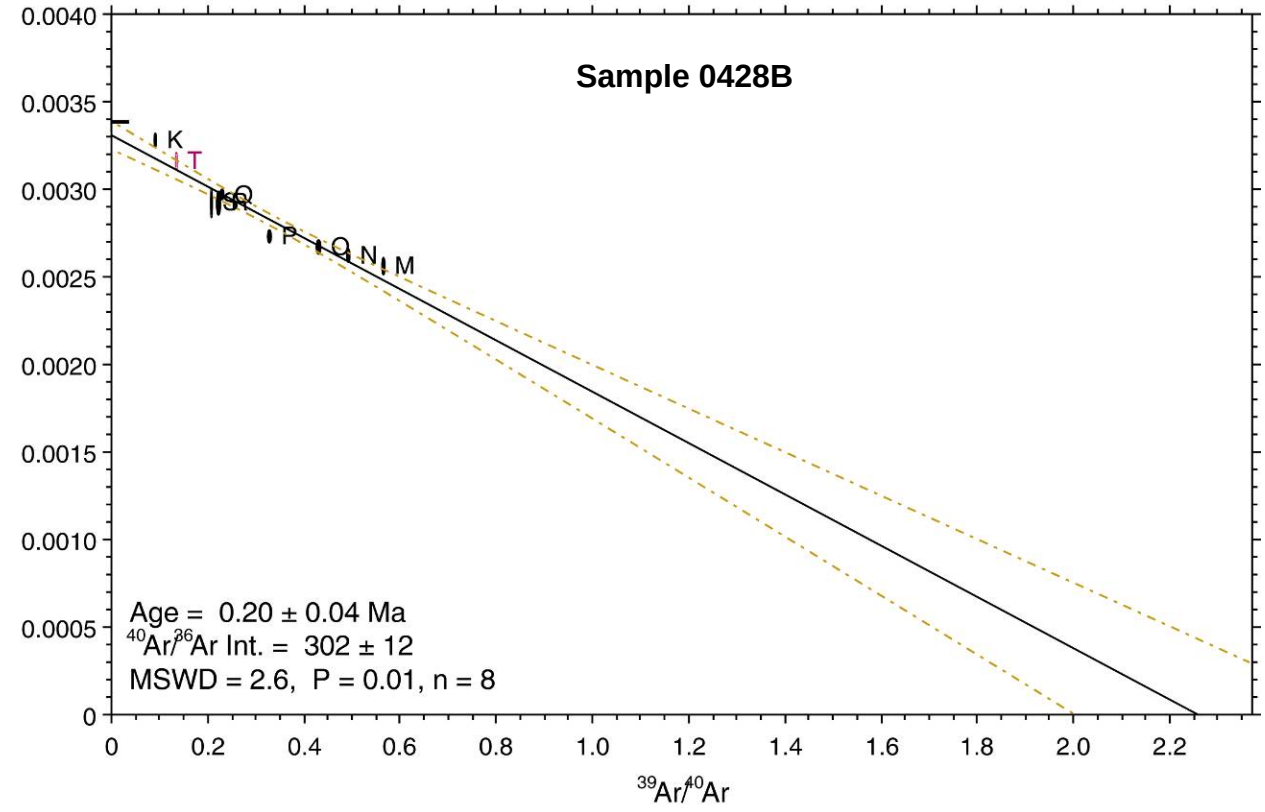

Figure DR 4a. Plateau and isochron results from the $^{40}Ar/^{39}Ar$ experiment on Clarks Butte lava flow sample 0428B.

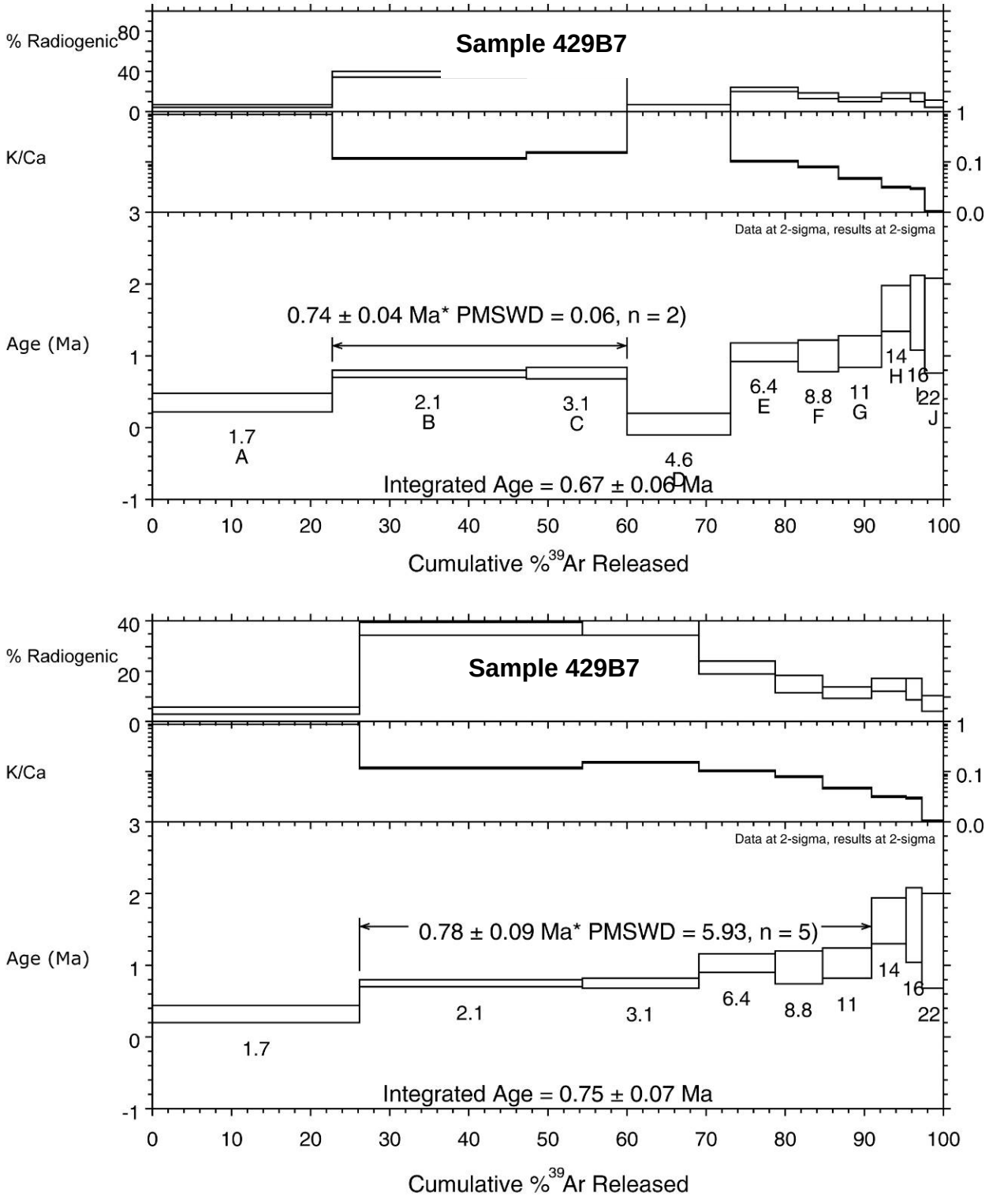

Figure DR 4b. Plateau results from the $^{40}Ar/^{39}Ar$ experiment on Deer Park lava flow sample 429B7. The D step was eliminated from the bottom graph, under the assumption that it has some unknown but significant error. The remaining steps yield an apparent age of 0.78±0.10 Ma, which agrees with the inverse isochron age of 0.7±0.2 Ma and was used in the weighted mean calculation of the age.

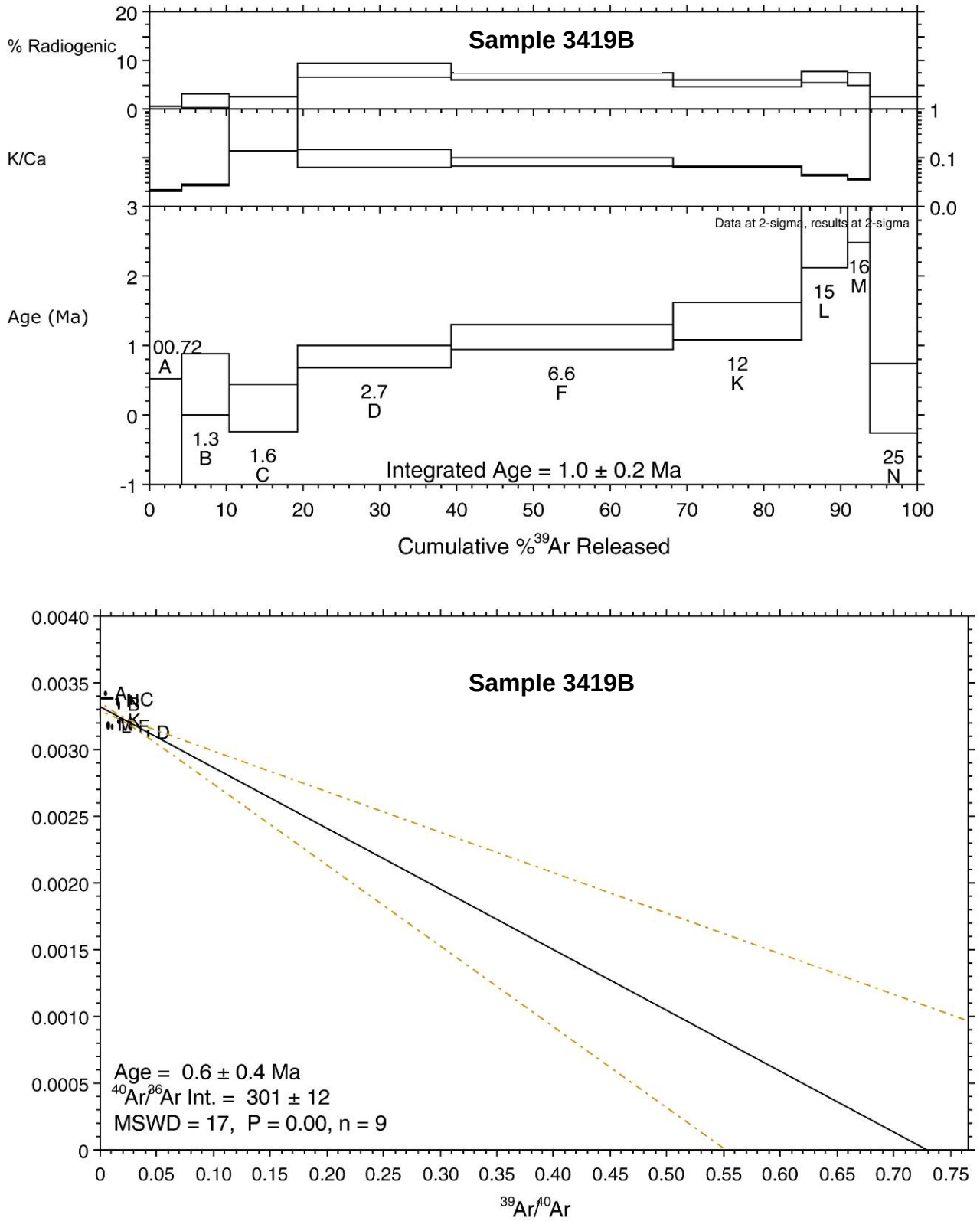

Figure DR 4d. Plateau and isochron results from the $^{40}Ar/^{39}Ar$ experiment on lower Bogus lava flow, Bogus Point sample 3419B.

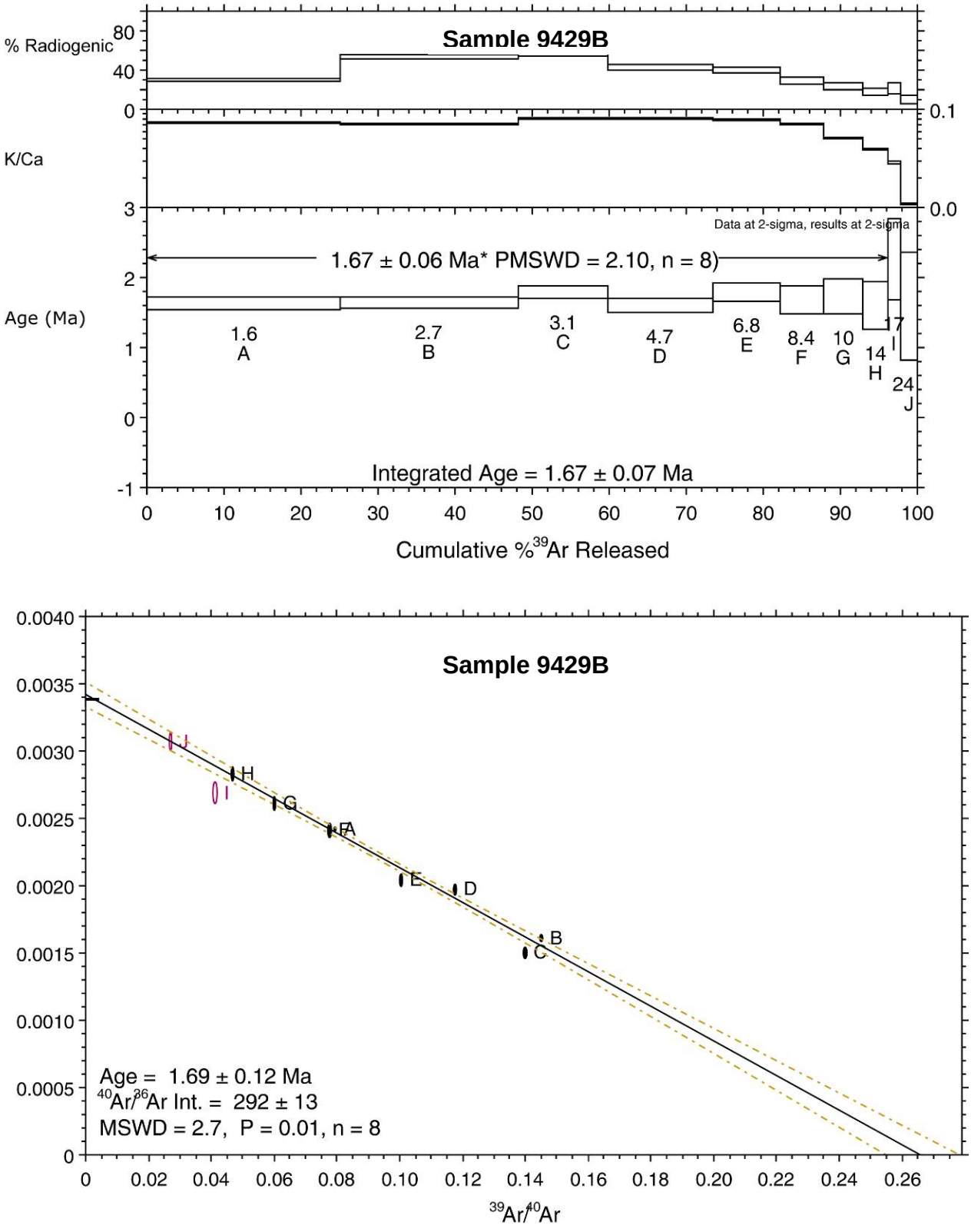

Figure DR 4e. Plateau and isochron results from the $^{40}Ar/^{39}Ar$ experiment on uppermost unit of lower Bogus lava flow, sample 9429B.

$^{40}Ar/^{39}Ar$ Analytical Results of Samples Processed at University of Nevada Las Vegas

Samples analyzed by the $^{40}Ar/^{39}Ar$ method at the University of Nevada Las Vegas were wrapped in Al foil and stacked in 6 mm inside diameter sealed fused silica tubes. Individual packets averaged 3 mm thick and neutron fluence monitors (FC-2, Fish Canyon Tuff sanidine) were placed every 5-10 mm along the tube. Synthetic K-glass and optical grade CaF_2 were included in the irradiation packages to monitor neutron induced argon interferences from K and Ca. Loaded tubes were packed in an Al container for irradiation. Samples irradiated at the Oregon State University Radiation Center were in-core for 7 hours in the In-Core Irradiation Tube (ICIT) of the 1 MW TRIGA type reactor. Correction factors for interfering neutron reactions on K and Ca were determined by repeated analysis of K-glass and CaF_2 fragments. Measured $(^{40}Ar/^{39}Ar)_K$ values were 1.56 (± 45.3%) x 10^{-2}. Ca correction factors were $(^{36}Ar/^{37}Ar)_{Ca}$ = 2.5292 (± 2.74%) x 10^{-4} and $(^{39}Ar/^{37}Ar)_{Ca}$ = 6.856 (± 1.27%) x 10^{-4}. J factors were determined by fusion of 3-8 individual crystals of neutron fluence monitors which gave reproducibility's of 0.1% to 0.45% at each standard position. An error in J of 0.1648% was used in age calculations. No significant neutron flux gradients were present within individual packets of crystals as indicated by the excellent reproducibility of the single crystal flux monitor fusions.

Irradiated crystals together with CaF_2 and K-glass fragments were placed in a Cu sample tray in a high vacuum extraction line and were fused using a 20 W CO_2 laser. Sample viewing during laser fusion was by a video camera system and positioning was via a motorized sample stage. Samples analyzed by the furnace step heating method utilized a double vacuum resistance furnace similar to the Staudacher et al. (1978) design. Reactive gases were removed by three GP-50 SAES getters prior to being admitted to a MAP 215-50 mass spectrometer by expansion. The relative volumes of the extraction line and mass spectrometer allow 80% of the gas to be admitted to the mass spectrometer for laser fusion analyses and 76% for furnace heating analyses. Peak intensities were measured using a Balzers electron multiplier by peak hopping through 7 cycles; initial peak heights were determined by linear regression to the time of gas admission. Mass spectrometer discrimination and sensitivity was monitored by repeated analysis of atmospheric argon aliquots from an on-line pipette system. Measured $^{40}Ar/^{36}Ar$ ratios were 281.73 ± 0.57% during this work, thus a discrimination correction of 1.04891 (4 AMU) was applied to measured isotope ratios. The sensitivity of the mass spectrometer was ~6 x 10^{-17} mol mV^{-1} with the multiplier operated at a gain of 45 over the Faraday. Line blanks averaged 2.2 mV for mass 40 and 0.03 mV for mass 36 for laser fusion analyses and 13.10 mV for mass 40 and 0.04 mV for mass 36 for furnace heating analyses. Discrimination, sensitivity, and blanks were relatively constant over the period of data collection. Computer automated operation of the sample stage, laser, extraction line and mass spectrometer as well as final data reduction and age calculations were done using LabSPEC software written by B. Idleman (Lehigh University). An age of 27.9 Ma (Steven et al., 1967; Cebula et al., 1986) was used for the Fish Canyon Tuff sanidine flux monitor in calculating ages for samples. All analytical data were reported at the confidence level of 1σ (standard deviation).

Complications arose in the application of the $^{40}Ar/^{39}Ar$ analytical procedure at the University of Nevada Las Vegas on the young basalt samples from this study. The results of some of these analyses were inconsistent with field relations and other ages or had analytical uncertainties that deemed them of minimal value for geologic interpretation. For these reasons, several of the $^{40}Ar/^{39}Ar$ ages were excluded from the weighted mean calculations of the lava flows. The isochron age for sample OWY-35 on the Clarks Butte lava flow was selected over the plateau age because it had a lower analytical error. The large analytical error for sample OWY-12 (173 ± 145 ka) and the unrealistically old age of 7 ± 1 Ma for sample OWY-13 on the Saddle Butte flows contradict the known stratigraphic and geologic position of these units. On the West Crater flow, the isochron value of 7 ± 8.5 ka for sample OWY-22 contradicts the ages derived from all other geochronological methods. The large analytical uncertainty on the isochron age of 120 ± 130 ka for OWY-23 indicates problems with the analysis. Sample OWY-36 was excluded from the weighted mean calculation of the age of the West Crater flow because of our low confidence in the reliability of the $^{40}Ar/^{39}Ar$ total gas analytical procedure.

Table DR 7a . $^{40}Ar/^{39}Ar$ Analytical Results, University of Nevada Las Vegas Isotope Geochronology Laboratory

Sample OWY-12, Saddle Butte 1 lava flow; groundmass, 95.70 mg, J = 0.0020992 ± 0.1648%

4 amu discrimination = 1.04891 ± 0.57%, 40/39K = 0.01560 ± 45.3%, 36/37Ca = 0.00025292 ± 2.74%, 39/37Ca = 0.0006856 ± 1.27%

step	T (C)	t (min.)	^{36}Ar	^{37}Ar	^{38}Ar	^{39}Ar	^{40}Ar	$\%^{40}Ar^*$	% ^{39}Ar rlsd	Ca/K	$^{40}Ar^*/^{39}ArK$	Age (ka)	1s.d.
1	550	12	2.642	105.890	4.095	87.648	742.63	4.2	12.8	9.586997663	506.686971	1307	186
2	610	12	0.883	146.318	1.548	63.728	216.97	5.4	9.3	18.26653349	196.854773	624	96
3	680	12	2.594	516.247	2.165	115.28	604.49	1.6	16.8	35.81215294	87.119329	303	168
4	750	12	1.644	599.000	2.171	142.3	313.996	1.8	20.8	33.64183367	38.725063	141	126
5	820	12	0.847	256.475	1.266	85.87	173.643	2.2	12.5	23.80149981	39.868403	145	104
6	895	12	0.757	187.740	0.817	49.839	160.409	-1.2	7.3	30.07418174	-30.655514	-120	-127
7	970	12	0.695	112.966	0.556	31.201	161.425	-1.4	4.6	28.89577449	-57.717007	-233	-179
8	1040	12	0.873	78.745	0.584	24.202	221.122	-0.4	3.5	25.9446541	-34.100976	-134	-207
9	1110	12	2.618	277.810	1.279	45.48	677.419	2.2	6.6	49.04113923	459.366831	1218	428
10	1170	12	1.820	480.325	0.564	15.447	391.074	1.6	2.3	265.5234177	617.079738	1499	1065
11	1240	12	2.656	1089.640	0.647	15.685	470.697	1.2	2.3	657.4301848	598.451138	1468	2381
12	1310	12	0.835	245.358	0.215	4.43	171.22	2.6	0.6	504.1110674	2998.679136	3585	1917
13	1400	12	0.763	229.182	0.189	4.54	149.951	-2.7	0.7	453.4328751	-370.013239	-2705	-1782
						Cumulative $\%^{39}Ar$ rlsd =			100.0		Total gas age =	452.8	94.1
note: isotope beams in mV, rlsd = released, error in age includes J error, all errors 1 sigma											Plateau age =	173.0	144.8
(^{36}Ar through ^{40}Ar are measured beam intensities, corrected for decay for the age calculations)											(steps 3-5)		
											No isochron		

Table DR 7b . $^{40}Ar/^{39}Ar$ Analytical Results, University of Nevada Las Vegas Isotope Geochronology Laboratory

Sample OWY-13, Saddle Butte 2 lava flow; groundmass, 97.00 mg, J = 0.002081 ± 0.1783%

4 amu discrimination = 1.04891 ± 0.57%, 40/39K = 0.01560 ± 45.3%, 36/37Ca = 0.00025292 ± 2.74%, 39/37Ca = 0.0006856 ± 1.27%

step	T (C)	t (min.)	^{36}Ar	^{37}Ar	^{38}Ar	^{39}Ar	^{40}Ar	$\%^{40}Ar^*$	% ^{39}Ar rlsd	Ca/K	$^{40}Ar^*/^{39}ArK$	Age (Ma)	1s.d.
1	550	12	70.638	124.374	15.327	45.96	20085.4	1.1	6.6	21.87993732	4.964896	18.54	9.42
2	600	12	24.652	132.969	5.394	43.031	7116.62	3.0	6.2	25.00734074	5.015492	18.73	3.63
3	650	12	23.926	317.506	5.552	83.812	6812.43	2.3	12.0	30.70975994	1.936617	7.26	1.78
4	700	12	19.983	427.057	4.785	99.851	5385.83	2.9	14.3	34.7118058	1.564490	5.86	1.28
5	750	12	16.288	296.998	4.293	102.74	4657.26	3.2	14.7	23.38433595	1.470434	5.51	0.99
6	810	12	12.791	167.241	34.309	82.667	3712.91	4.3	11.9	16.33024456	1.929396	7.23	0.98
7	880	12	9.640	141.128	2.678	60.749	2820.07	5.2	8.7	18.76591909	2.416635	9.05	1.01
8	960	12	7.282	112.928	2.000	39.772	2143.26	5.9	5.7	22.96466909	3.196276	11.96	1.18
9	1060	12	5.710	147.129	2.041	57.921	1659.28	5.7	8.3	20.52981509	1.620344	6.07	0.62
10	1160	12	4.370	749.588	1.729	53.423	1081.96	4.7	7.7	116.6298178	0.959328	3.60	0.59
11	1400	12	3.980	1828.550	1.008	26.597	689.347	6.9	3.8	661.0964158	2.020867	7.57	2.33
						Cumulative $\%^{39}Ar$ rlsd =			100.0		Total gas age =	8.31	0.62
note: isotope beams in mV, rlsd = released, error in age includes J error, all errors 1 sigma											Plateau age =	7.03	1.00
(^{36}Ar through ^{40}Ar are measured beam intensities, corrected for decay for the age calculations)											(steps 3-7)		
											No isochron		

Table DR 7c . $^{40}Ar/^{39}Ar$ Analytical Results, University of Nevada Las Vegas Isotope Geochronology Laboratory

Sample OWY-22, upper West Crater lava flow; groundmass, 193.80 mg, J = 0.0020478 ± 0.2002%

4 amu discrimination = 1.04891 ± 0.57%, 40/39K = 0.01560 ± 45.3%, 36/37Ca = 0.00025292 ± 2.74%, 39/37Ca = 0.0006856 ± 1.27%

step	T (C)	t (min.)	^{36}Ar	^{37}Ar	^{38}Ar	^{39}Ar	^{40}Ar	$\%^{40}Ar^*$	% ^{39}Ar rlsd	Ca/K	$^{40}Ar^*/^{39}ArK$	Age (ka)	1s.d.
1	550	12	1.836	192.980	23.716	455.41	746.175	1.7	6.2	3.42551036	17.634511	64	36
2	600	12	1.128	337.651	18.115	566.76	235.32	1.0	7.7	4.81795039	3.804272	14	32
3	650	12	1.442	665.003	19.468	958.12	247.23	2.0	13.0	5.614374377	4.623321	17	32
4	700	12	1.399	692.886	17.282	1097.5	229.711	2.1	14.8	5.106306758	3.804272	14	31
5	750	12	1.058	395.353	15.956	1048.1	210.931	1.9	14.2	3.04886134	3.531558	13	28
6	810	12	0.981	269.066	16.486	1113.9	239.135	9.3	15.1	1.951761678	18.195733	66	27
7	880	12	0.878	148.101	12.844	804.89	231.952	7.3	10.9	1.486581597	19.038734	69	27
8	960	12	0.766	89.592	7.329	432.17	198.974	2.4	5.8	1.674960869	9.566321	35	28
9	1060	12	1.046	194.712	5.941	356.93	261.414	7.0	4.8	4.411155818	47.956167	169	33
10	1160	12	2.424	1087.450	7.098	368.31	424.943	5.9	5.0	24.01438895	68.247231	236	33
11	1400	12	5.749	2238.350	4.093	196.25	1074.16	3.6	2.7	94.70505525	243.154027	729	338
						Cumulative $\%^{39}Ar$ rlsd =			100.0		Total gas age =	69.86	19.15
note: isotope beams in mV, rlsd = released, error in age includes J error, all errors 1 sigma											Plateau age =	37.60	21.01
(^{36}Ar through ^{40}Ar are measured beam intensities, corrected for decay for the age calculations)											(steps 1-8)		
											Isochron age =	7.0	8.5
											(steps 2-5)		

Table DR 7d . $^{40}Ar/^{39}Ar$ Analytical Results, University of Nevada Las Vegas Isotope Geochronology Laboratory

Sample OWY-23, lower West Crater lava flow; groundmass, 194.50 mg, J = 0.002026 ± 0.2048%

4 amu discrimination = 1.04891 ± 0.57%, 40/39K = 0.01560 ± 45.3%, 36/37Ca = 0.00025292 ± 2.74%, 39/37Ca = 0.0006856 ± 1.27%

step	T (C)	t (min.)	^{36}Ar	^{37}Ar	^{38}Ar	^{39}Ar	^{40}Ar	$\%^{40}Ar^*$	$\%\ ^{39}Ar$ rlsd	Ca/K	$^{40}Ar^*/^{39}ArK$	Age (ka)	1s.d.
1	550	12	12.439	205.453	5.291	239.04	3546.66	2.8	4.0	7.084138787	657.096150	1527	314
2	600	12	5.054	353.054	6.746	480.46	1376.77	3.3	8.0	6.054709832	103.687660	344	70
3	650	12	5.786	680.669	14.380	1093.2	1519.73	3.9	18.2	5.129170691	57.255971	198	42
4	700	12	7.462	794.362	17.226	1311.9	1970.08	3.3	21.8	4.987748609	51.485138	179	44
5	750	12	7.006	398.380	13.102	965.16	1911.43	1.7	16.0	3.398351584	35.118652	124	50
6	810	12	5.655	243.782	9.563	649.45	1570.35	2.1	10.8	3.090211119	49.675360	173	55
7	880	12	3.421	173.661	5.590	389.21	933.258	1.5	6.5	3.67387957	37.174053	131	58
8	960	12	3.567	146.512	3.917	240.17	1001.34	3.7	4.0	5.025012195	176.305012	551	94
9	1060	12	3.315	207.955	4.339	261.83	907.428	3.3	4.3	6.545188641	124.913357	407	81
10	1160	12	3.260	1001.330	4.434	241.74	686.096	5.2	4.0	34.4188377	166.354045	524	129
11	1400	12	6.272	2701.700	3.031	148.93	1082.6	3.1	2.5	156.1556402	293.125389	841	536
						Cumulative $\%^{39}Ar$ rlsd =			100.0		Total gas age =	292	39
note: isotope beams in mV, rlsd = released, error in age includes J error, all errors 1 sigma											Plateau age =	182	42
(^{36}Ar through ^{40}Ar are measured beam intensities, corrected for decay for the age calculations)											(steps 2-7)		
											Isochron age =	120	130
											(steps 2-7)		

Table DR 7e. $^{40}Ar/^{39}Ar$ Analytical Results, University of Nevada Las Vegas Isotope Geochronology Laboratory

Sample OWY-35, Clarks Butte lava flow; groundmass, 95.60 mg, J = 0.001934 ± 0.2652%

4 amu discrimination = 1.04891 ± 0.57%, 40/39K = 0.01560 ± 45.3%, 36/37Ca = 0.00025292 ± 2.74%, 39/37Ca = 0.0006856 ± 1.27%

step	T (C)	t (min.)	^{36}Ar	^{37}Ar	^{38}Ar	^{39}Ar	^{40}Ar	$\%^{40}Ar^*$	% ^{39}Ar rlsd	Ca/K	$^{40}Ar^*/^{39}ArK$	Age (ka)	1s.d.
1	600	12	1.912	96.633	4.124	217.6	537.92	5.4	6.0	3.795506002	145.381552	447	55
2	650	12	2.851	161.512	7.576	508.35	805.40	5.7	14.0	2.714560777	97.279167	311	41
3	700	12	3.123	194.041	8.481	608.2	886.187	6.3	16.7	2.725849535	99.325748	317	40
4	750	12	1.109	113.990	5.948	443.97	314.594	10.8	12.2	2.193295112	75.538724	246	29
5	810	12	1.000	81.814	4.558	315.14	276.142	6.6	8.7	2.217752913	55.201696	183	31
6	880	12	1.210	94.415	4.247	282.87	330.849	5.2	7.8	2.851860436	59.979627	198	35
7	960	12	1.086	119.560	4.352	296.25	293.967	7.9	8.1	3.448850621	75.210336	245	33
8	1060	12	1.470	194.394	6.276	391.93	388.179	7.2	10.8	4.239621853	70.957813	232	34
9	1160	12	2.559	590.360	8.953	433.97	602.639	7.4	11.9	11.65368594	108.966974	345	51
10	1400	12	5.328	1129.61	3.821	142.92	1220.07	2.6	3.9	68.85865766	281.437808	784	278
						Cumulative $\%^{39}Ar$ rlsd =			100.0		Total gas age =	301.09	24.30
note: isotope beams in mV, rlsd = released, error in age includes J error, all errors 1 sigma											Plateau age =	247.60	24.91
(^{36}Ar through ^{40}Ar are measured beam intensities, corrected for decay for the age calculations)											(steps 2-10)		
											Isochron age =	179	21
											(steps 1-4)		

Table DR 7f. $^{40}Ar/^{39}Ar$ Analytical Results, University of Nevada Las Vegas Isotope Geochronology Laboratory

Sample OWY-36, lower West Crater lava flow; groundmass, 97.40 mg, J = 0.0019025 ± 0.3522%

4 amu discrimination = 1.04891 ± 0.57%, 40/39K = 0.01560 ± 45.3%, 36/37Ca = 0.00025292 ± 2.74%, 39/37Ca = 0.0006856 ± 1.27%

step	T (C)	t (min.)	36Ar	37Ar	38Ar	39Ar	40Ar	%40Ar*	% 39Ar rlsd	Ca/K	40Ar*/39ArK	Age (ka)	1s.d.
1	550	12	2.113	73.828	4.876	126.55	580.386	1.8	4.5	5.078413	83.504943	266	96
2	600	12	0.990	96.832	4.136	200.374	250.86	0.8	7.1	4.205656	9.110004	31	36
3	650	12	3.541	226.343	7.194	450.004	961.83	1.9	15.8	4.37753	42.099130	139	50
4	700	12	9.338	253.965	8.333	493.976	2654.78	3.6	17.4	4.474649	230.920483	657	113
5	750	12	0.986	146.284	5.646	422.427	238.95	-0.1	14.9	3.012639	-6.370853	-22	-28
6	810	12	0.898	87.466	3.594	266.979	226.155	-1.1	9.4	2.849988	-8.381704	-29	-31
7	880	12	0.967	86.516	2.646	189.529	250.414	1.6	6.7	3.972344	19.283274	65	46
8	960	12	1.112	94.647	2.421	166.337	295.584	4.0	5.9	4.953028	68.169827	220	43
9	1060	12	1.220	122.174	3.347	215.819	315.943	2.6	7.6	4.927636	35.840108	119	44
10	1160	12	2.078	596.969	3.995	221.749	423.455	1.7	7.8	23.56362	31.808794	106	85
11	1400	12	5.374	1406.830	21.830	88.283	1130.14	1.1	3.1	144.4735	169.404889	504	525
							Cumulative %39Ar rlsd =		100.0		Total gas age =	194.41	27.35
note: isotope beams in mV, rlsd = released, error in age includes J error, all errors 1 sigma											No plateau		
(36Ar through 40Ar are measured beam intensities, corrected for decay for the age calculations)											No isochron		

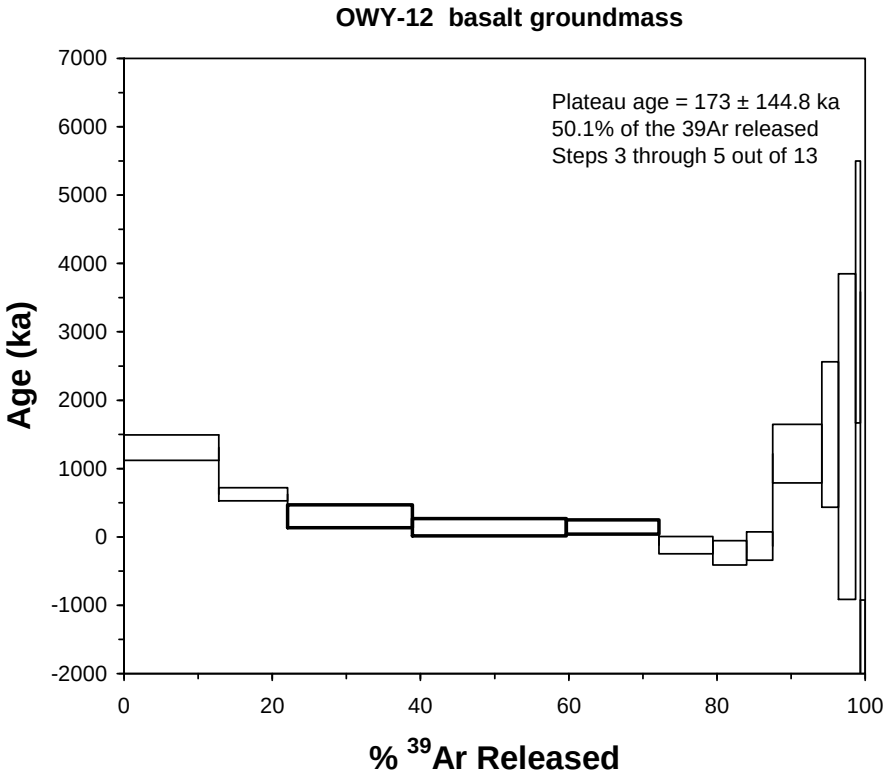

Figure DR 5a. Plateau results from the $^{40}Ar/^{39}Ar$ experiment on Saddle Butte 1 lava flow sample OWY-12 (no isochron).

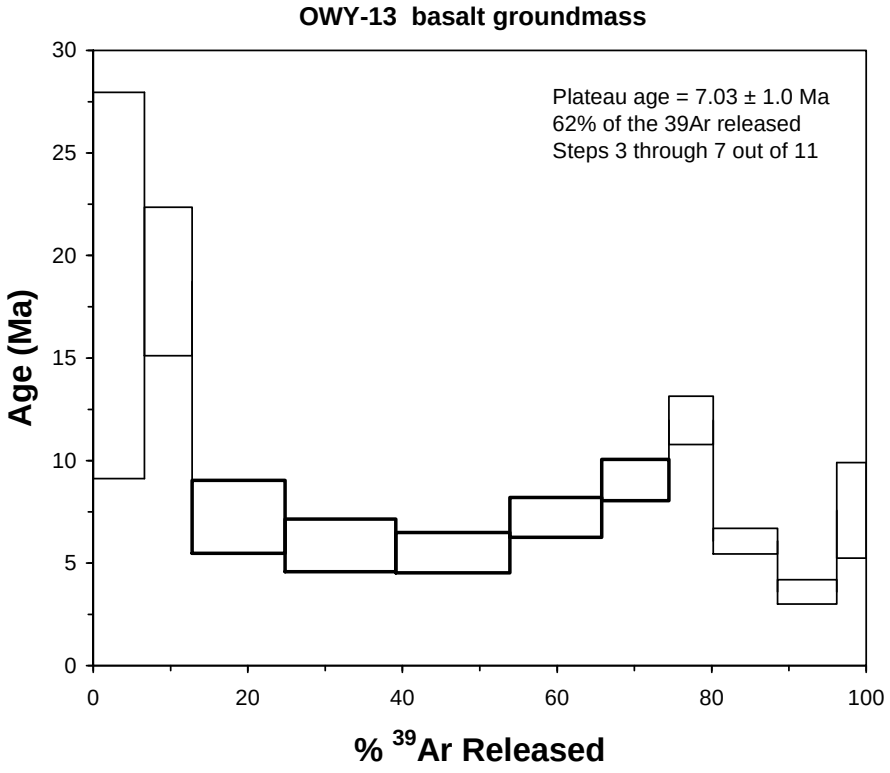

Figure DR 5b. Plateau results from the $^{40}Ar/^{39}Ar$ experiment on Saddle Butte 2 lava flow sample OWY-13 (no isochron).

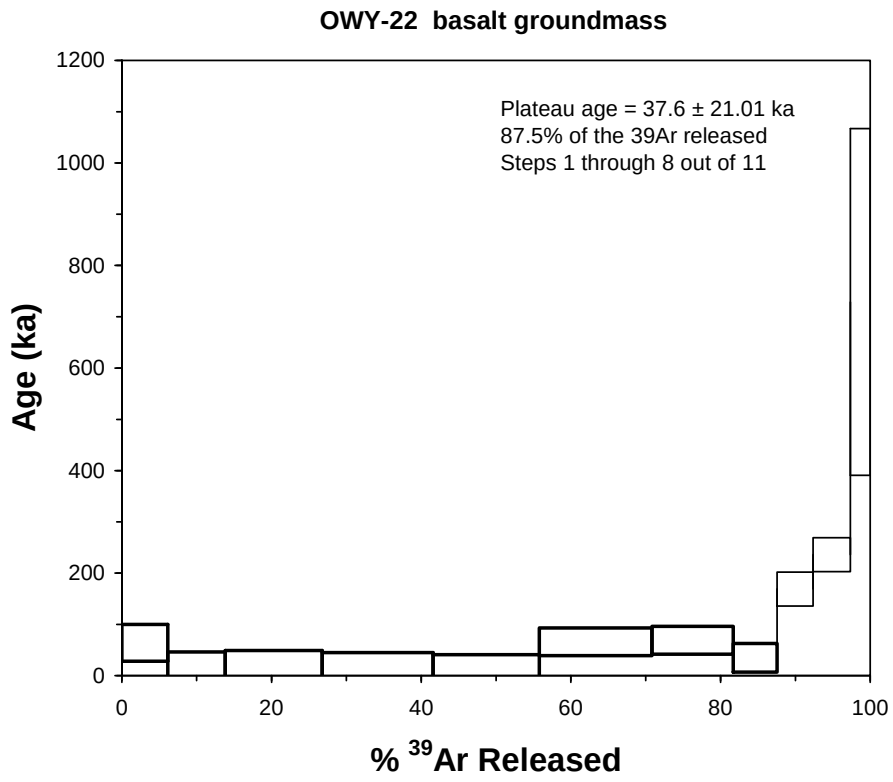

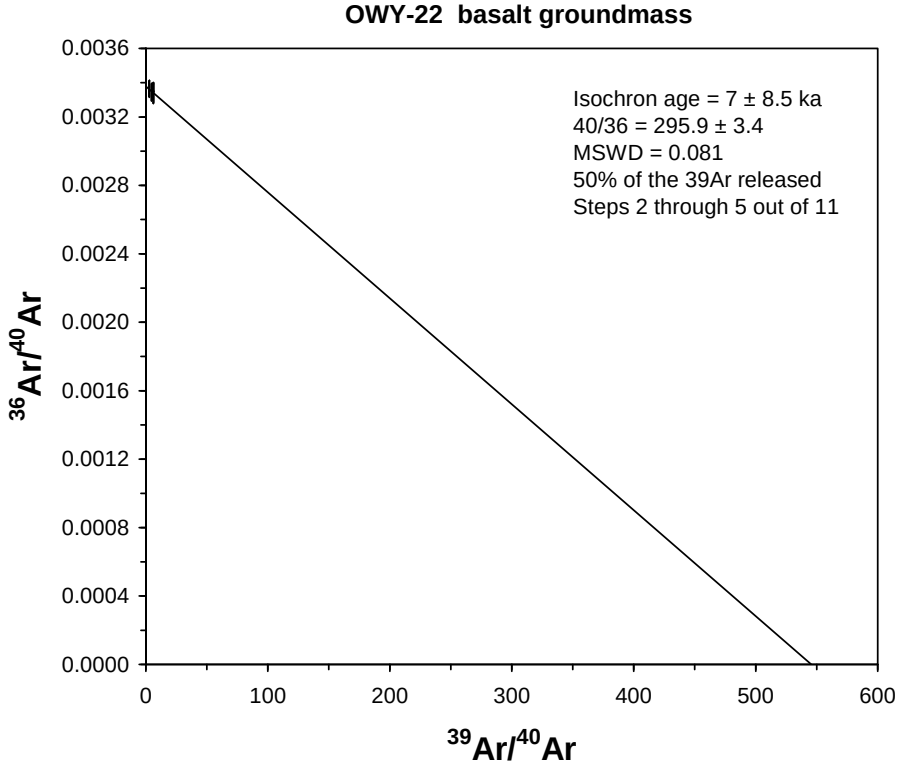

Figure DR 5c. Plateau and isochron results from the $^{40}Ar/^{39}Ar$ experiment on lower West Crater lava flow sample OWY-22.

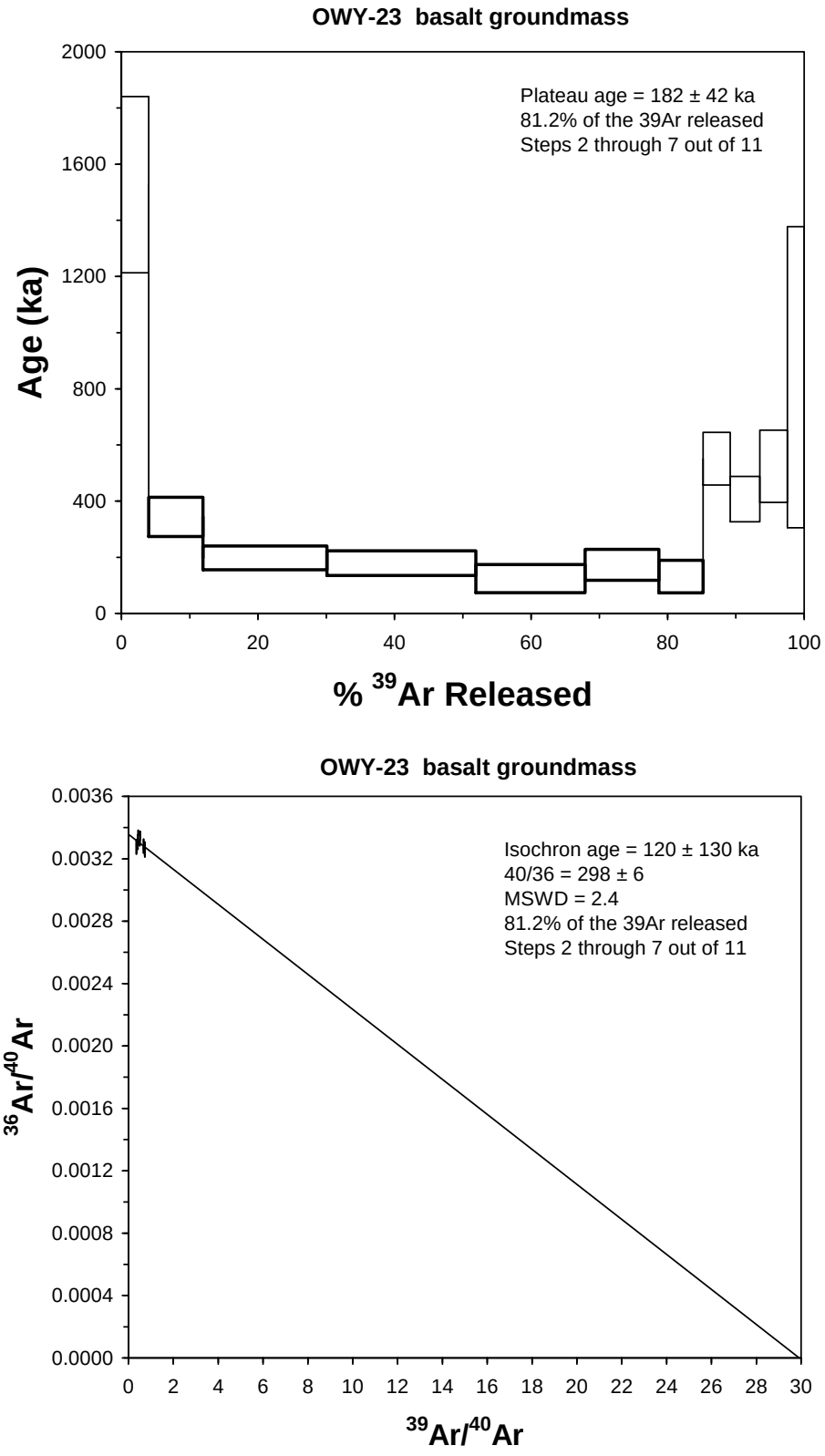

Figure DR 5d. Plateau and isochron results from the $^{40}Ar/^{39}Ar$ experiment on upper West Crater lava flow sample OWY-23.

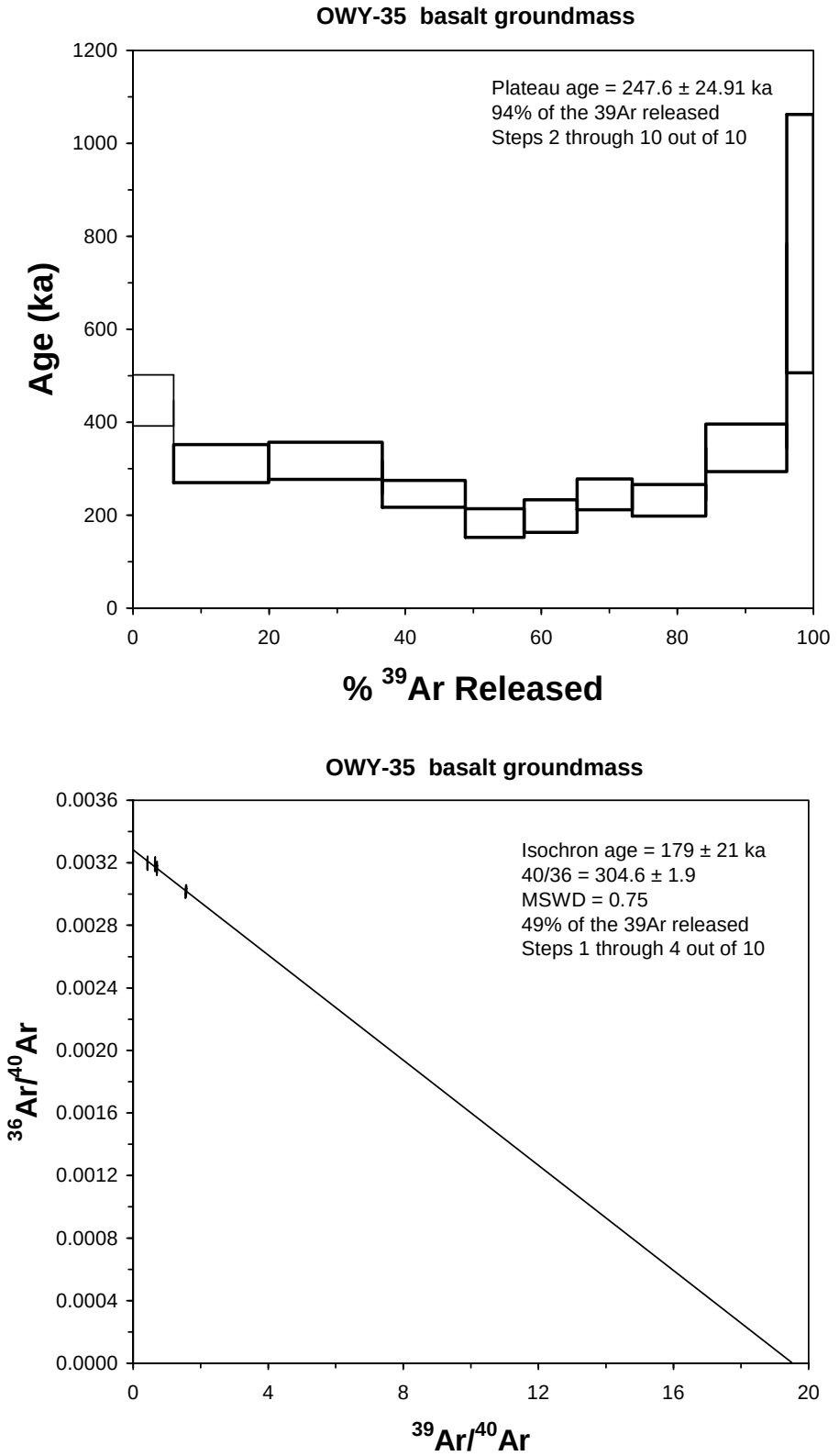

Figure DR 5e. Plateau and isochron results from the $^{40}Ar/^{39}Ar$ experiment on Clarks Butte lava flow sample OWY-35.

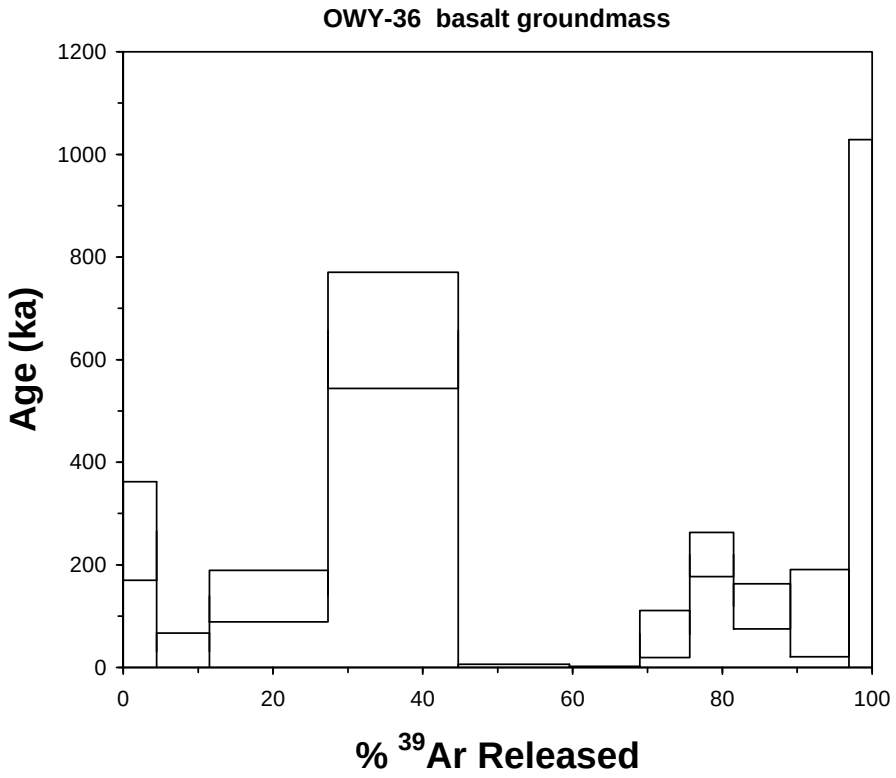

Figure DR 5f. Total gas results from the $^{40}Ar/^{39}Ar$ experiment on lower West Crater lava flow sample OWY-36. No plateau or isochron.

Data Repository References

Bondre, N. R., 2006, Field and geochemical investigation of basaltic magmatism in the western United States and western India [Ph.D. thesis]: Oxford, Miami University, 263 p.

Bondre, N. R., and Hart, W. K., 2006, Source and process effects on basaltic volcanism in the Jordan Valley Volcanic Field, southeastern Oregon: Abstracts with Programs Geological Society of America, v. 38, no. 7, p. 446.

Bondre, N. R., and Hart, W. K., 2004, Flow chemistry and vent alignments from the Jordan Valley volcanic field, Oregon; insights into the evolution of monogenetic volcano fields: Abstracts with Programs Geological Society of America, v. 36, no. 4, p. 75.

Brereton, N.R., 1970, Corrections for interfering isotopes in the $^{40}Ar/^{39}Ar$ dating method: Earth and Planetary Science Letters, v. 8, p. 427-433.

Brossy, C.C., 2007, Fluvial response to intra-canyon lava flows, Owyhee River, southeastern Oregon: M.S. Thesis, Central Washington University, 109 p.

Butler, R. F., 1992, Paleomagnetism: Magnetic domains to geologic terranes: Boston, Blackwell Scientific Publications, 319 p.

Cebula, G.T., M.J. Kunk, H.H. Mehnert, C.W. Naeser, J.D. Obradovich, and J.F. Sutter, 1986, The Fish Canyon Tuff, a potential standard for the 40Ar-39Ar and fission-track dating methods: Terra Cognita (6th Int. Conf. on Geochronology, Cosmochronology and Isotope Geology), v. 6, p. 139.

Cerling, T. E., 1990, Dating geomorphologic surfaces using cosmogenic ^{3}He: Quaternary Research, v. 33, p. 148.

Cerling, T. E., and Craig, H., 1994, Geomorphology and in-situ cosmogenic isotopes: Annual Review of Earth & Planetary Sciences, v. 22, p. 273-317.

Cerling, T. E., Poreda, R. J., and Rathburn, S. L., 1994, Cosmogenic ^{3}He and ^{21}Ne age of the Big Lost River flood, Snake River Plain, Idaho: Geology, v. 22, p. 227.

Cerling, T. E., Webb, R. H., Poreda, R. J., Rigby, A. D., and Melis, T. S., 1999, Cosmogenic ^{3}He ages and frequency of late Holocene debris flows from Prospect Canyon, Grand Canyon, USA: Geomorphology, v. 27, p. 93.

Champion, D.E., 1980, Holocene Geomagnetic secular variation in the western United States: Implications for the global geomagnetic field, *U.S. Geological Survey Open-File Report* 80-824, 326p.

Champion, D. E., and Shoemaker, E. M., 1977, Paleomagnetic evidence for episodic volcanism on the Snake River Plain, National Aeronautics and Space Administration Technical Memorandum, p. 7-9.

Clynne, M.A., Calvert, A.T., Wolfe, E.W., Evart, R.C., Fleck, R.J., and Lanphere, M.A., 2008, The Pleistocene eruptive history of Mount St. Helens, Washington, from 300,000-12,800 years before present: U.S. Geological Survey Professional Paper 1750, p. 593-627.

Dalrymple, G.B., Lanphere, M.A., 1969, Potassium-Argon Dating, W.H. Freeman and Company, San Francisco, 258pp.

Dalrymple, G.B., Lanphere, M.A., 1974. $^{40}Ar/^{39}Ar$ age spectra of some undisturbed terrestrial samples: Geochimica et Cosmochimica Acta, v. 38, p. 715-738.

Davis, J.O., 1985, Correlation of late Quaternary tephra layers in a long pluvial sequence near Summer Lake, Oregon: Quaternary Research, v. 23, p. 38-53.

Deino, A.L., and McBrearty, S., 2002, $^{40}Ar/^{39}Ar$ dating of the Kapthurin Formation, Baringo, Kenya, Jour. Human Evol., v. 42, p. 185-210.

Fenton, C. R., Webb, R. H., Cerling, T. E., Poreda, R. J., and Nash, B. P., 2002, Cosmogenic He ages and geochemical discrimination of lava-dam outburst-flood deposits in western Grand Canyon, Arizona, *in* House, P. K., Webb, R. H., Baker, R. V., and Levish, D. R., eds., Ancient floods and modern hazards: Principles and applications of paleoflood hydrogeology, AGU Water and Science Applications no. 5: Washington, D.C., American Geophysical Union, p. 191-215.

Fenton, C. R., Cerling, T. E., Poreda, R. J., Nash, B. P., and Webb, R. H., 2004, Geochemical discrimination of five Pleistocene lava-dam outburst-flood deposits, western Grand Canyon, Arizona: Journal of Geology, v. 112, no. 1, p. 91-110.

Fenton, C. R., Webb, R. H., and Cerling, T. E., 2006, Peak discharge of a Pleistocene lava-dam outburst flood in Grand Canyon, Arizona, USA: Quaternary Research, v. 65, no. 2, p. 324-335.

Fenton, C.R., Niedermann, S., Goethals, M.M., Schneider, B., and Wijbrans, J., 2009. Evaluation of cosmogenic ^{3}He and ^{21}Ne production rates in olivine and pyroxene from two Pleistocene basalt flows, western Grand Canyon, AZ, USA: Quaternary Geochronology, v. 4, p. 475-492.

Fleck, R.J., Sutter, J.F., Elliot, D.H., 1977, Interpretation of discordant $^{40}Ar/^{39}Ar$ age-spectra of Mesozoic tholeiites from Antarctica, Geochimica et Cosmochimica Acta, v. 41, p. 15–32.

Gosse, J. C., and Phillips, F. M., 2001, Terrestrial in situ cosmogenic nuclides: Theory and application: Quaternary Science Reviews, v. 20, no. 14, p. 1475-1560.

Hart, W. K., 1982, Geochemical, geochronologic and isotopic significance of low K, high-alumina olivine tholeiite in the northwestern Great Basin, U.S.A. [Ph.D. thesis]: Cleveland, Ohio, Case Western Reserve University, 410 p.

Hart, W. K., Aronson, J. L., and Mertzman, S. A., 1984, Areal distribution and age of low-K, high-alumina olivine tholeiite magmatism in the northwestern Great Basin: Geological Society of America Bulletin v. 95, p. 186-195.

Hart, W. K., and Mertzman, S. A., 1983, Late Cenozoic volcanic stratigraphy of the Jordan Valley area, southeastern Oregon: Oregon Geology, v. 45, no. 2, p. 15-19.

Kato, S., Danaher, T., Hart, W. K., and WoldeGabriel, G., 1999, Use of sodium polytungstate solution in the purification of volcanic glass shards for bulk chemical analysis: Nature and Human Activities, v. 4, p. 45-54.

Kuntz, M. A., Champion, D. E., Spiker, E. C., and Lefebvre, R. H., 1986, Contrasting magma types and steady-state, volume-predictable, basaltic volcanism along the Great Rift, Idaho: Geological Society of America Bulletin, v. 97, p. 579-594.

Kurz, M. M., 1986, In situ production of terrestrial cosmogenic helium and some applications to geochronology: Geochimica et Cosmochimica Acta, v. 50, p. 2855.

Lal, D., 1991. Cosmic ray labeling of erosion surfaces: in situ nuclide production rates and erosion models: Earth and Planetary Science Letters, v. 104, p. 424–439.

McElhinny, M. W., 1973, Palaeomagnetism and plate tectonics, Cambridge Earth Science Series: London, Cambridge University Press, 358 p.

McIntosh, W.C., Heizler, M., Peters, L., and Esser, R., 2003, $^{40}Ar/^{39}Ar$ geochronology at the New Mexico Bureau of Geology and Mineral Resources: New Mexico Bureau of Geology and Mineral Resources Open File Report OF-AR-1, 10 p.

Mertzman, S. A., 2000, K-Ar results from the southern Oregon-northern California Cascade Range: Oregon Geology, v. 62, no. 4, p. 99-122.

Renne, P.R., Swisher, C.C., Deino, A.L., Karner, D.B., Owens, T.L., and DePaolo, D.J., 1998, Intercalibration of standards, absolute ages and uncertainties in $^{40}Ar/^{39}Ar$ dating: Chemical Geology, v. 145, p. 117-152.

Negrini, R.M., Erbes, D.B., Faber, K., Herrera, A.M., Roberts, A.P., Cohen, A.S., Wigand, P.E., and Foit, F.F., 2000, A paleoclimate record for the past 250,000 years from summer Lake, Oregon, USA: I. Chronology and magnetic proxies for lake level: Journal of Paleolimnology, v. 24, p. 125-149.

Shoemaker, K. A., 2004, The tectonomagmatic evolution of the Late Cenozoic Owyhee Plateau, northwestern United States [Ph.D. thesis]: Oxford, Miami University, 288 p.

Shoemaker, K. A., and Hart, W. K., 2002, Temporal controls on basalt genesis and evolution on the Owyhee Plateau, Idaho and Oregon *in* Bonnichsen, B., White, C. M., and McCurry, M., eds., Tectonic and Magmatic Evolution of the Snake River Plain Province: Idaho Geological Survey Bulletin 30, p. 313-328.

Staudacher, T.H., Jessberger, E.K., Dorflinger, D., and Kiko, J., 1978, A refined ultrahigh-vacuum furnace for rare gas analysis: J. Phys. E: Sci. Instrum., v. 11, p. 781-784.

Steiger, R.H., and Jäger, E., 1977, Subcommission on geochronology: Convention on the use of decay constants in geo- and cosmochronology: Earth and Planetary Science Letters, v. 36, p. 359-362.

Steven, T.A., H.H. Mehnert, and J.D. Obradovich, 1967, Age of volcanic activity in the San Juan Mountains, Colorado, U.S. Geol. Surv. Prof. Pap., 575-D, p. 47-55.

Taylor, J.R., 1997, An Introduction to Error Analysis: The Study of Uncertainties in Physical Measurements, 2nd edition: University Science Books, 327pp.

Turrin, B.D., Gutman, J.T., and Swisher III, C.C., 2008, A 13 ± 3ka age determination of a tholeiite, Pinacate volcanic field, Mexico, and improved methods for $^{40}Ar/^{39}Ar$ dating of young basaltic rocks: Journal Volcan. Geotherm. Res., v. 177, p. 848-856.

Vermeesch, P., 2007. CosmoCalc: an Excel add-in for cosmogenic nuclide calculations: Geochem. Geophys. Geosyst., v. 8, Q08003. doi:10.1029/2006GC001530.

Wendt, I., and Carl, C., 1991, The statistical distribution of the mean squared weighted deviation: Chemical Geology, v. 86, p. 275-285.